UNIVERSITY OF LJUBLJANA

Faculty of Civil and Geodetic Engineering

Institute of Structural Engineering,
Earthquake Engineering and Construction IT
1001 Ljubljana, Jamova 2, P.O. Box 3422, Slovenia
Phone (+386 61) 176 85 00, 125 07 05
Fax (+386 61) 125 06 93, 125 06 81

CAMUS INTERNATIONAL BENCHMARK
Report on numerical modelling

IKPIR Report EE - 1/98

Ljubljana, February 1998

Matej Fischinger
Tatjana Isaković
Samo Križaj
Tomaž Vidic

1. INTRODUCTION

Buildings with structural walls are frequently used in Slovenia, in particular for apartment buildings. Similar structures behaved well during the 1979 Montenegro earthquake. It has been realised, however, that there are still a number of unsolved problems in the design of structural walls. This is also reflected in the present version of Eurocode 8/1.3 where still some ambiguities regarding the design of walls (e.g. minimum thickness, reinforcement distribution, ductility requirements, and the design for shear) exist. To solve these problems additional experimental as well as numerical work is needed. Since the present capability of realistic and practical modelling of non-linear static and dynamic seismic response of RC structural walls is still limited, this benchmark study is a great opportunity to improve our knowledge.

At the University of Ljubljana, we have got some experience in using macro models in the analysis of the seismic response of structural walls. Macro models consist of a finite number of discrete springs following a certain force-displacement relationship. They attempt to describe the overall behaviour by means of an appropriate idealisation. In the presented study a multiple-vertical-line element MVLEM (e. g. Fischinger, Vidic, Fajfar, 1992; the paper is enclosed at the end of the report) is used (see section 2). The element was incorporated into the standard DRAIN-2D program, which is readily available for engineering community. The first version of the program was published as early as in 1973 (Kanaan, Powell, 1973).

The main objective of the study is to check the ability of the chosen element and the standard computer code to model the global parameters of the response (e.g. maximum displacement, ultimate strength, and basic features of the specific behaviour of walls, such as uplift of the tension corner and rocking). It is realised, however, that by the definition the macro models can not reflect the details of the response, such as stress-strain relationship, localised damage and details in time history. Nevertheless, it is believed that the data, which are usually available in earthquake engineering, are so crude that modelling of such details is frequently questionable by any model. According to our limited experience, the chosen element provides a proper balance between the simplicity of the model and accuracy of the global results and we hope that this will be confirmed by the benchmark study.

In this report, first the chosen wall model (Section 2) and computer code (Section 3) are introduced. After a short discussion of seismic loading (Section 4), the complete model of the wall is described (Section 5).
Main results of the analyses are given in Section 6. They include initial natural frequencies and modes (6.1), design using response spectrum analysis (6.2), non-linear static analysis (6.3) and non-linear time-history analysis (6.4). The results that are submitted on diskettes for further comparisons are called 'the results of the basic analysis' in this report.
Several comparative analyses were made to study individual parameters of the chosen model (e.g. damping, reinforcement pull-out, sequence of loading, different model). Results are discussed in Section 7 and conclusions are made in Section 8.

2. MULTIPLE-VERTICAL-LINE ELEMENT MODEL (MVLEM)

In the model (Figure 1), several vertical springs are connected by rigid beams at the top and bottom level. They simulate axial and flexural behaviour of the wall segment (Figure 2, Figure 3). Horizontal spring is modelling shear behaviour (Figure 2, Figure 3). Elastic shear behaviour was assumed in this study. The model is described in more detail in the enclosed paper at the end of this report.

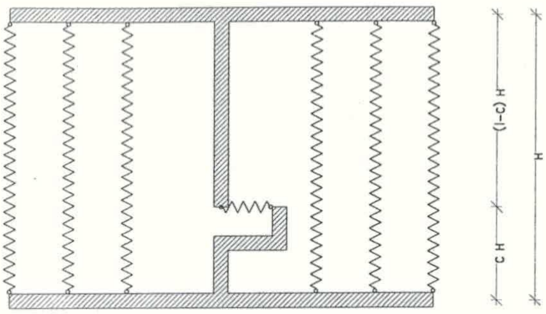

Figure 1: MVLE Model

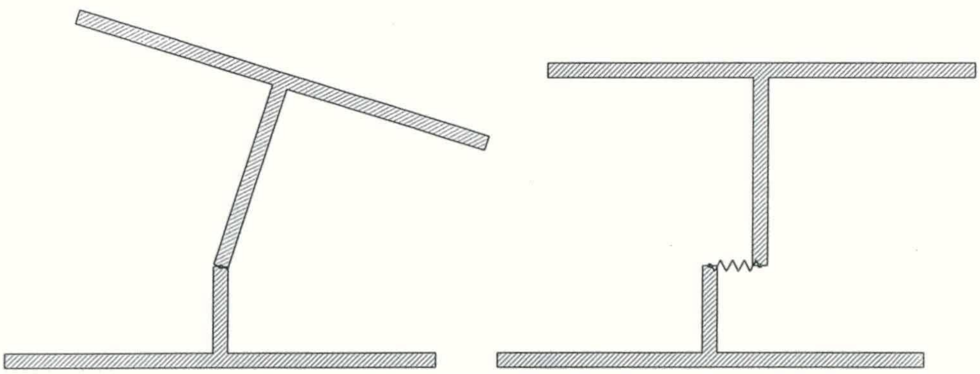

Figure 2: Flexural and shear behaviour

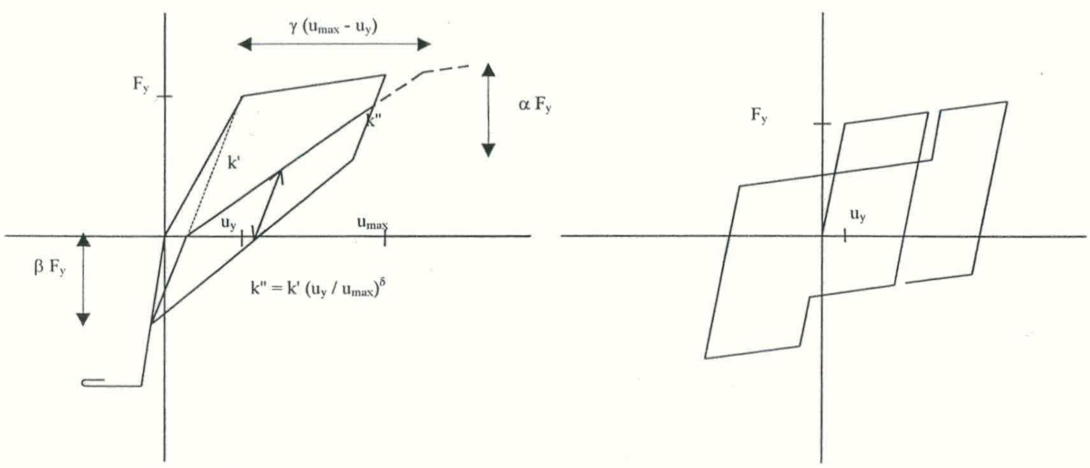

Figure 3: Axial and shear spring properties

3. "DRAIN-2D" COMPUTER CODE

DRAIN-2D program is a standard computer code for inelastic time history analysis of 2D structures which has been most frequently used by the earthquake engineering community for the last two decades (Kanaan, Powell, 1973). It uses relatively simple numerics, based on the constant acceleration within the time interval. There is no iteration within the integration time step and the correction forces are applied at the beginning of the next interval.

The element library includes a number of different (macro) elements. Most of them are of the beam-column type. Such elements can not model some of the basic features of the inelastic response of structural walls (e.g. uplift of the tension edge). Therefore a new RC wall-type element, based on the multiple vertical spring representation was added to DRAIN-2D at the University of Ljubljana (Section 2). Some other modifications to enable inelastic cyclic static analysis were made. A beam-column element with three-linear Takeda hysteretic rules was also incorporated into the program.

4. EARTHQUAKE LOADING

The three specified signals (CAMUS02, CAMUS17, and CAMUS 19) were used in the time history analyses. The elastic spectra for the three records are given in Figure 4 - Figure 6, respectively. The shape of the spectra is quite different (Figure 7). The sharp peak of the CAMUS02 spectrum near the first natural period of the wall is to be noted. It might have an important influence on the behaviour of the wall during the first test at the lowest level (0.24g) of excitation.

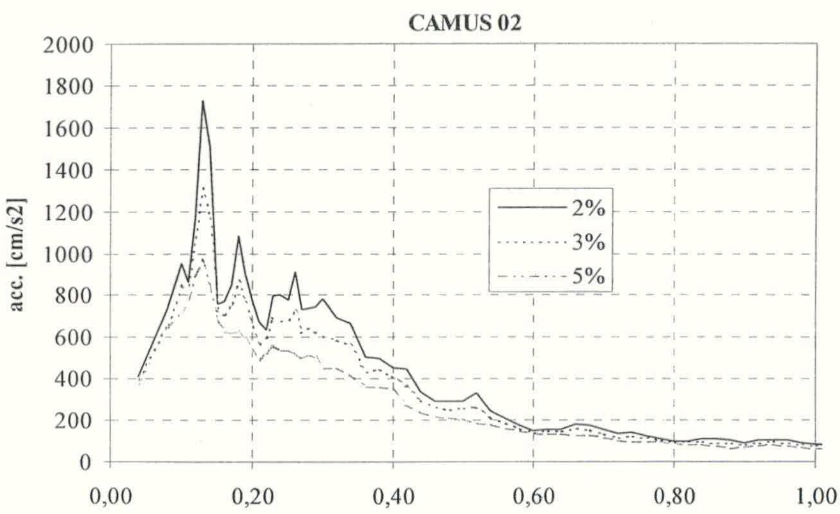

Figure 4: CAMUS 02 elastic spectra (2, 3 and 5% of critical damping)

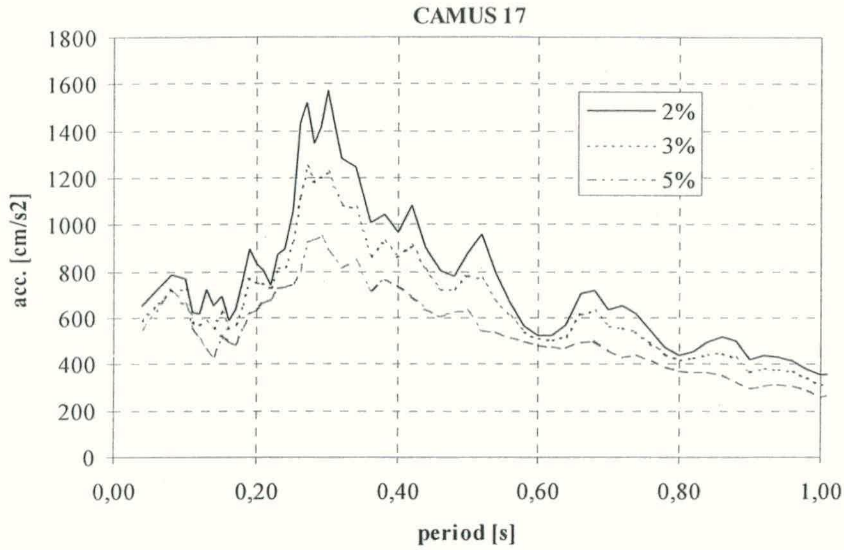

Figure 5: CAMUS 17 elastic spectra (2, 3 and 5% of critical damping)

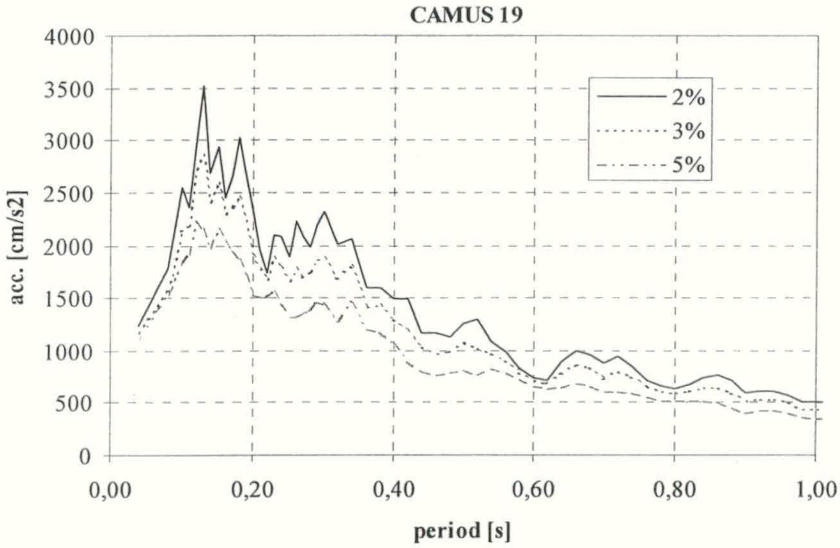

Figure 6: CAMUS 19 elastic spectra (2, 3 and 5% of critical damping)

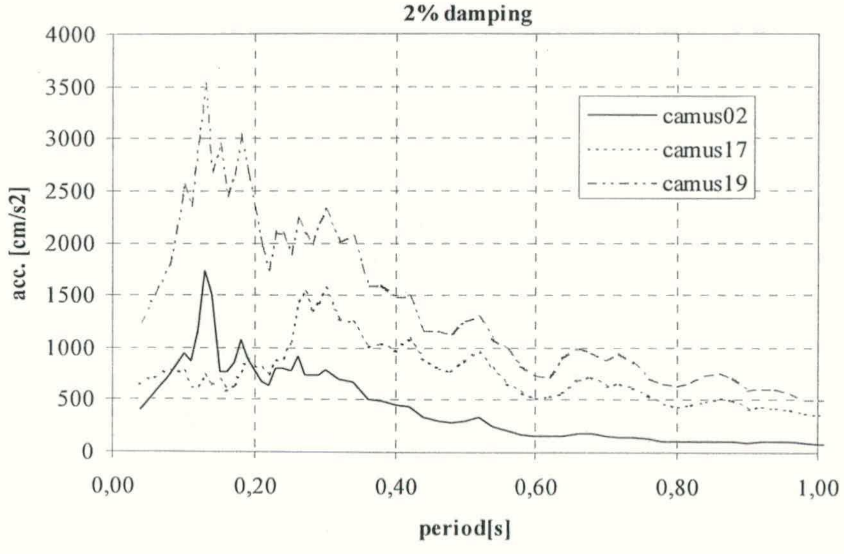

Figure 7: Elastic spectra at 2% damping

5. MODELLING OF THE WALL

5.1 Wall geometry (element mesh)

The wall was modelled as a stack of MVL elements (Figure 8). The changes in longitudinal reinforcement, the location of floors and the location of strain gages were considered in determining the mesh. More plastification was expected at the base (close to the foundation). Therefore, shorter elements were used there. It was proved later, however, that non-linear behaviour was not confined to the base only. Several checks were made and the density of the mesh was considered to be appropriate at upper levels, too.

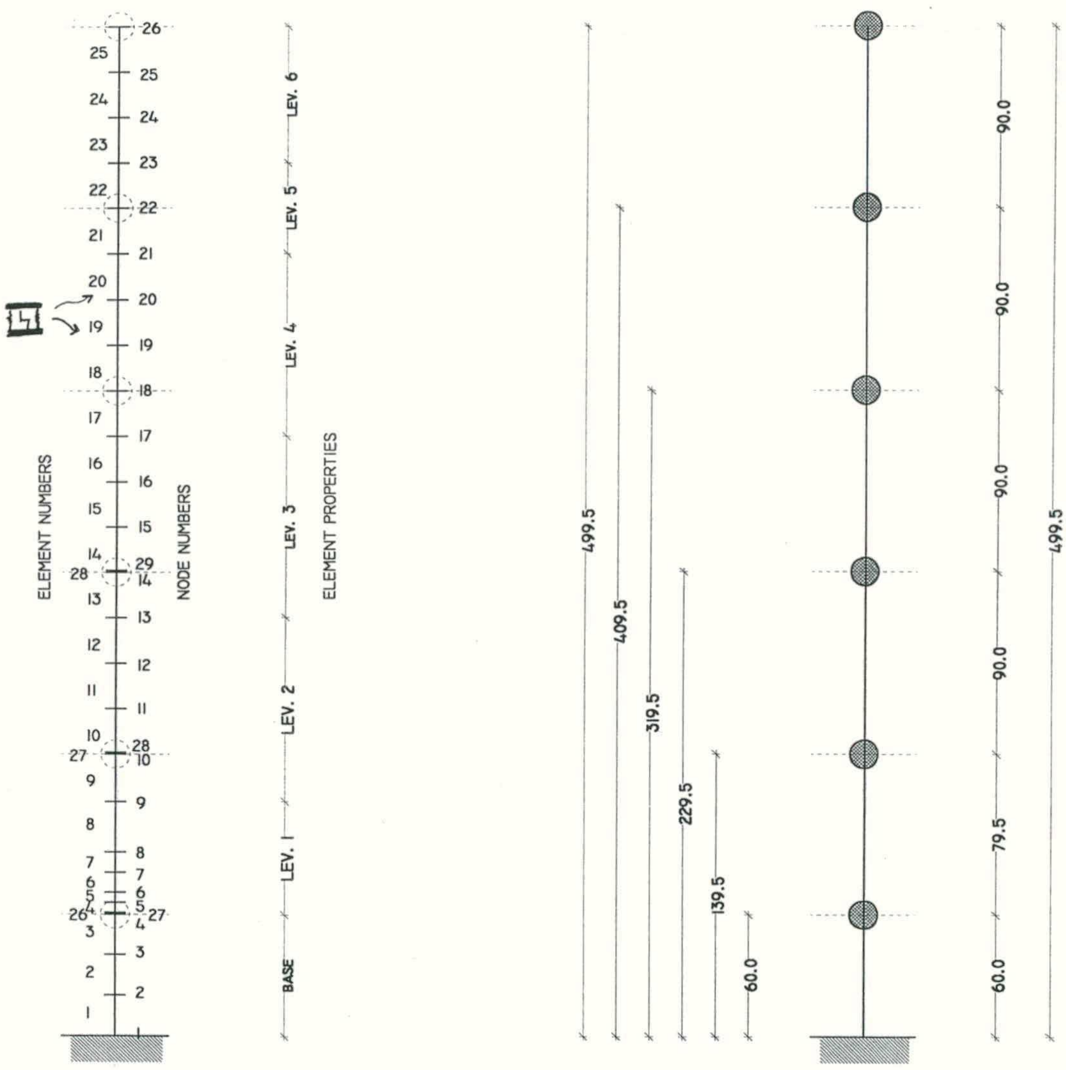

Figure 8: Wall model

5.2 Modelling of an individual MVLE

According to previous experience, 6 vertical springs were chosen for each MVLE. The appertaining areas of the cross section for each individual spring are shown in Figure 9 and Figure 10 for the wall section and footing, respectively. The horizontal spring was located at 30% of the height of the element.

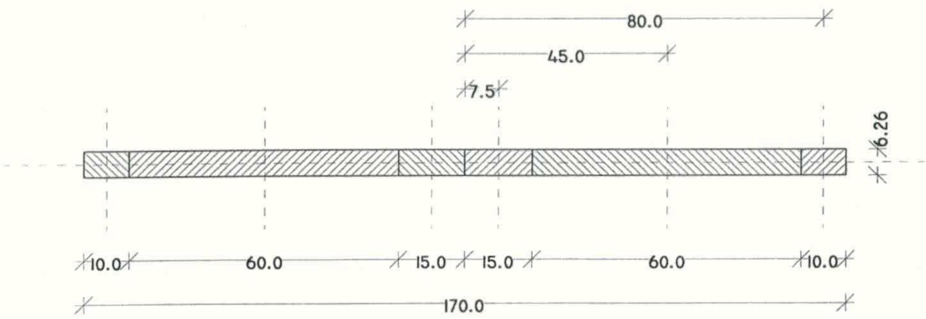

Figure 9: The appertaining areas of the wall cross section

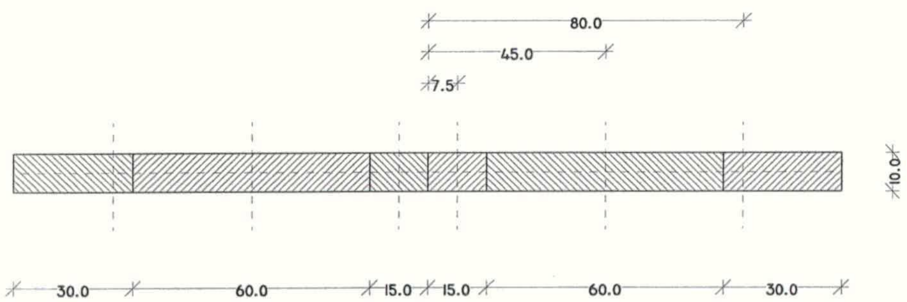

Figure 10: The appertaining areas of the base cross section

5.2.1 Modelling of vertical springs

Each vertical spring was modelled as RC truss element. Only the contribution of concrete was considered to determine the strength and stiffness in compression. Only the contribution of reinforcement was considered to determine the strength in tension (the two springs without reinforcement had no tensile strength). This supposition was considered acceptable at later phases of response. The contribution of both, concrete and reinforcement, was considered to determine the stiffness in tension. To determine this average stiffness, the energy criteria was used for outer springs and the geometric average for the central springs. The stiffness of the vertical springs is listed in Table 1.

Table 1 : Stiffness of the vertical springs

all units: kN, cm				stiffness			
level	spring loc.	el. length	type	comp.	tens.	hrd.	dy

			no.				
1	1	1,00	10	191.869,0	70.349,0	1216,0	1,71E-03
1	2	1,00	11	1.151.214,0	19.609,0	6,0	3,43E-05
1	3	1,00	12	287.804,0	64.723,0	291,0	5,04E-04
1	1	5,00	1	38.373,0	14.070,0	243,0	8,56E-03
1	2	5,00	2	230.243,0	3.922,0	1,0	1,72E-04
1	3	5,00	3	57.561,0	12.945,0	58,0	2,52E-03
1	1	10,00	4	19.187,0	7.035,0	122,0	1,71E-02
1	2	10,00	5	115.121,0	1.961,0	0,3	3,43E-04
1	3	10,00	6	28.780,0	6.421,0	29,0	5,04E-03
1	1	24,75	7	7.752,0	2.842,0	49,0	4,24E-02
1	2	24,75	8	46.514,0	792,0	0,3	8,49E-04
1	3	24,75	9	11.628,0	2.615,0	12,0	1,25E-02
2	1	1,00	16	191.869,0	52.000,0	793,0	1,54E-03
2	2	1,00	11	1.151.214,0	19.609,0	6,0	3,43E-05
2	3	1,00	17	287.804,0	64.723,0	291,0	5,04E-04
2	1	22,50	13	8.528,0	2.311,0	35,0	3,47E-02
2	2	22,50	14	51.165,0	871,0	0,3	7,72E-04
2	3	22,50	15	12.791,0	2.877,0	13,0	1,13E-02
3	1	1,00	29	191.869,0	42.760,0	397,0	9,38E-04
3	2	1,00	11	1.151.214,0	19.609,0	6,0	3,43E-05
3	3	1,00	30	287.804,0	57.747,0	232,0	4,50E-04
3	1	22,50	18	8.528,0	1.900,0	18,0	2,11E-02
3	2	22,50	14	51.165,0	871,0	0,3	7,72E-04
3	3	22,50	19	12.791,0	2.567,0	10,0	1,01E-02
4	1	22,50	20	8.528,0	1.500,0	5,0	8,84E-03
4	2	22,50	14	51.165,0	871,0	0,3	7,72E-04
4	3	22,50	21	12.791,0	2.165,0	7,0	8,89E-03
5	1	22,50	22	8.528,0	1.125,0	3,0	5,98E-03
5	2	22,50	14	51.165,0	871,0	0,3	7,72E-04
5	3	22,50	21	12.791,0	2.165,0	7,0	8,89E-03
6	1	22,50	22	8.528,0	1.125,0	3,0	5,98E-03
6	2	22,50	14	51.165,0	871,0	0,3	7,72E-04
6	3	22,50	23	12.791,0	436,0	0,3	1,54E-03
base	1	20,00	24	45.975,0	27.939,0	61,0	4,83E-03
base	2	20,00	25	91.950,0	1.239,0	0,3	5,43E-04
base	3	20,00	26	22.988,0	4.090,0	15,0	7,97E-03

Spring location:

- 1 → external
- 2 → middle
- 3 → internal

5.2.2 Modelling of horizontal (shear) springs

Elastic behaviour of shear springs was considered in the basic analysis.

5.3.3 Modelling of materials

<u>Concrete</u>

Average values for Young modulus E = 30650 MPa and shear modulus G = 12260 MPa were considered. Average concrete compression strength f_d = 35.2 MPa was taken into account. The behaviour of concrete in compression followed the vertical spring hysteretic rule (Figure 3). The tensile strength was neglected in the basic analysis.

Steel

Bilinear stress-strain relations were determined (Figure 11), based on the plots published in the benchmark report. 2% hardening after yielding was chosen and the published failure stress was considered. The yield stress was determined accordingly.

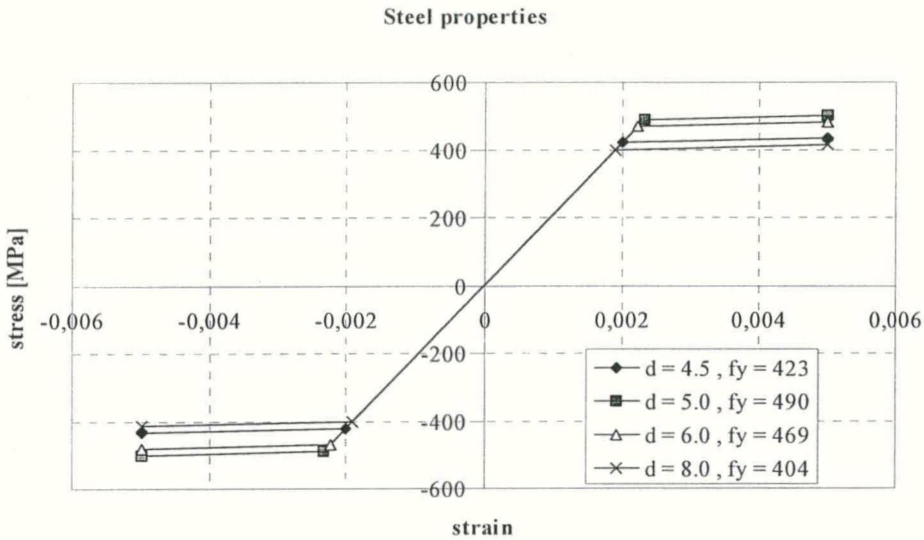

Figure 11 : Steel properties

5.3 Boundary conditions

Fixed support at the upper level of the shaking table was assumed in the basic analyses. The effect of pull-out of the longitudinal reinforcement from the footing was studied separately. Rocking of the table was not considered to be important for the results.

6. ANALYSIS AND RESULTS

Linear analyses (modal analysis as well as response spectrum analysis to check the design) and non-linear static, cyclic and time-history analysis were performed.

6.1 Initial natural frequencies and modes

First, the initial natural frequencies were calculated. The wall was modelled as a simple beam-column cantilever. The uncracked gross concrete sections were considered. Only the bending in-plane modes were evaluated. The results are given in Table 2 and Table 3. The calculated first natural frequency (9.46 Hz) was much lower than that, reported in the benchmark report (7.24 Hz). This most probably indicates a considerable pre-cracking of the wall. However, the information on pre-cracking is typically not available in advance. In addition, it could affect only the first stage of the

CAMUS02 response. Later, the wall cracked anyway. Therefore, we still decided to consider the uncracked sections at the beginning of the response-history analyses.

Table 2: Natural frequencies / periods

mode	period [s]	radial frequency [rad / s]	natural frequency [1/s]
1	0,106	59,42	9,46
2	0,023	277,69	44,20
3	0,011	591,40	94,12
4	0,007	868,04	138,15
5	0,006	1058,00	168,39
6	0,003	1924,03	306,22

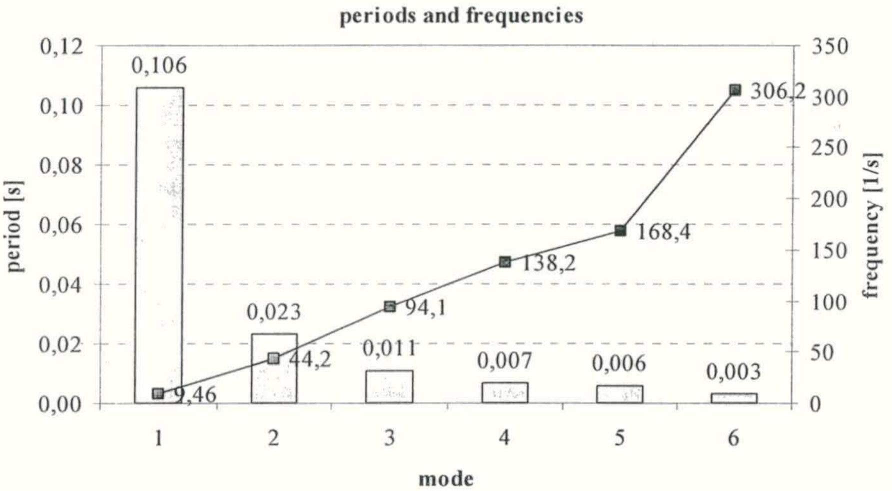

Figure 12 : Natural frequencies / periods

Table 2: Mode shapes

	mode shapes					
elevation [m]	1	2	3	4	5	6
0,000	0	0	0	0	0	0
0,600	0,017	0,166	0,309	0,357	0,214	1,000
1,365	0,101	0,659	1,000	0,934	0,475	-0,128
2,295	0,272	1,000	0,428	-0,796	-0,886	0,022
3,195	0,496	0,802	-0,693	-0,374	1,000	-0,001
4,095	0,746	0,081	-0,619	1,000	-0,701	0,001
4,995	1,000	-0,855	0,627	-0,472	0,234	0,000

6.2 Response spectrum analysis (redesign of the wall)

Repose spectrum analysis was made to estimate the design forces. French design response spectrum (Earthquake Regulations, 1992) for nominal ground acceleration 0.25 g was used (Figure 13). Parameters were estimated in such a way, that the calculated reinforcement approximately matched the reinforcement, published in the benchmark report.

It was observed that the wall was most probably designed with no seismic force reduction (behaviour factor q = 1.0). It was also observed (Figure 14), that the bending moment capacity closely followed the design demand over the entire height of the wall. This indicated the possibility of yielding in upper stories, too.

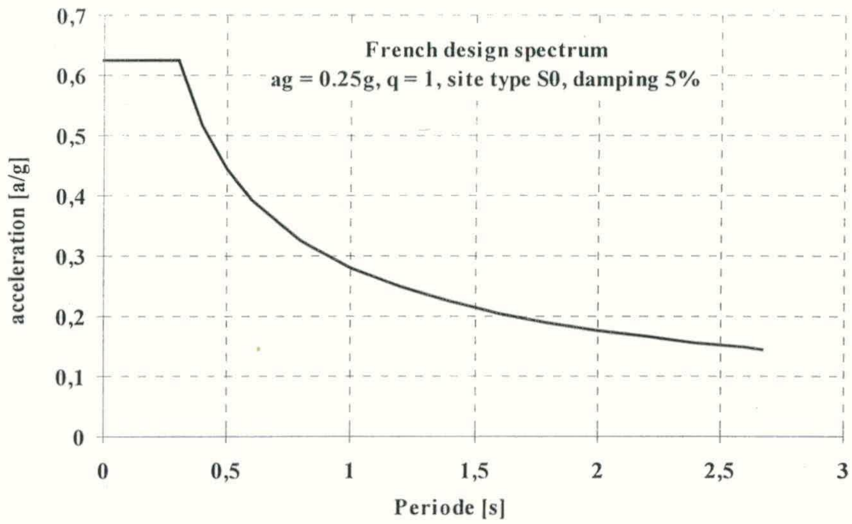

Figure 13: French design response spectrum

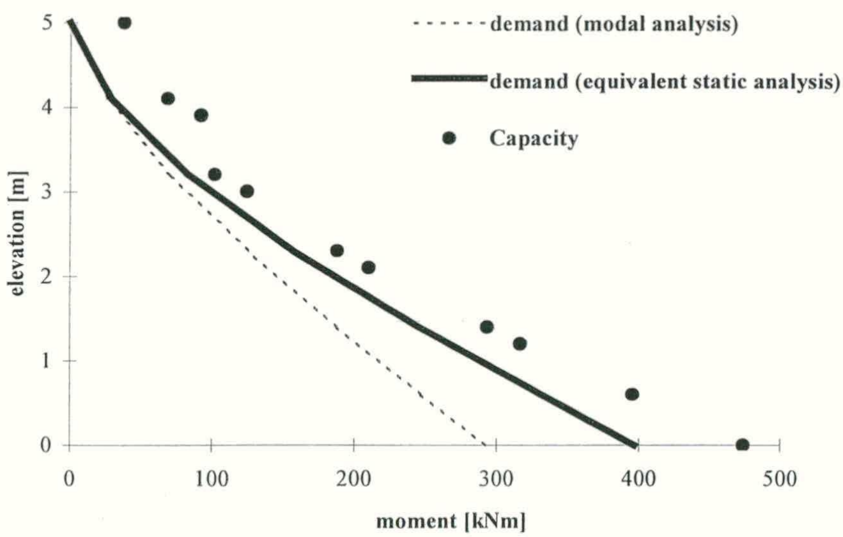

Figure 14: Bending moment capacity versus design demand

6.3 Non-linear static analyses

Non-linear monotonic static (push-over) analysis (Figure 15) as well as cyclic analysis (Figure 16) were made to estimate the strength and global behaviour of the wall. Inverted triangular distribution of horizontal forces over the height of the wall was considered. The uniform distribution was considered for comparison. In Figure 15 and

Figure 16 the top displacement (DX6) is plotted against base shear just above the footing (base of the 1st story of the wall).

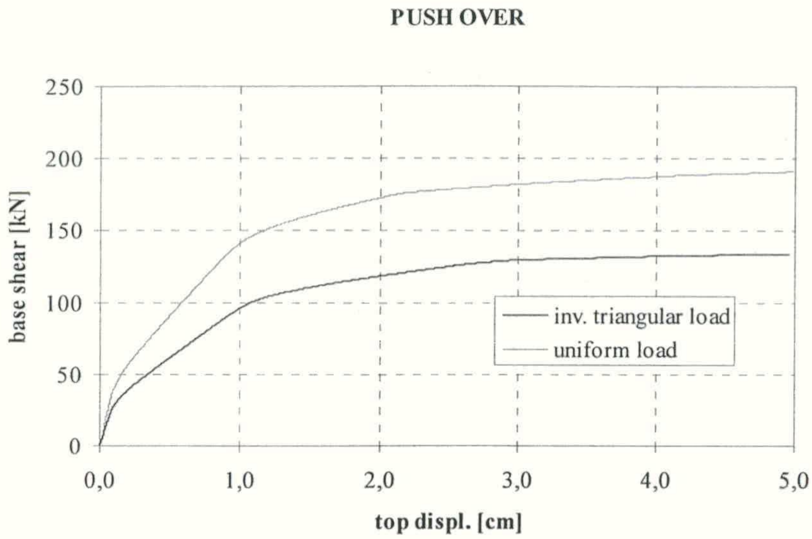

Figure 15: Push over analysis

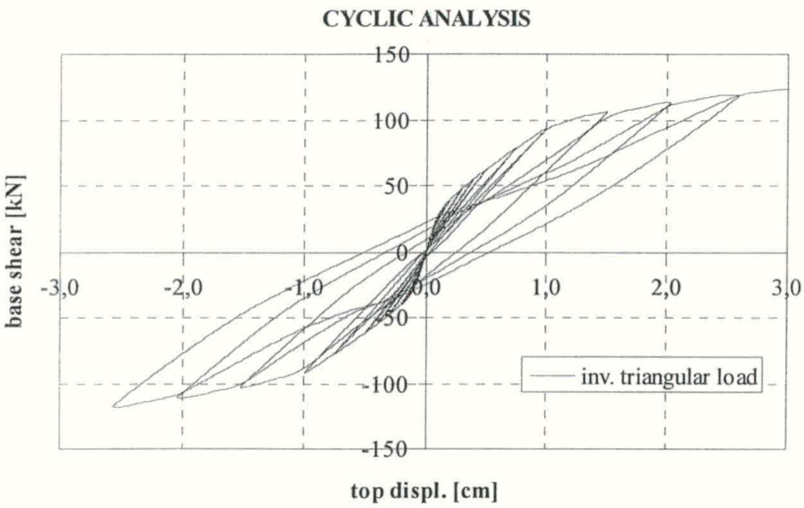

Figure 16: Cyclic analysis

6.4 Non-linear time-history analyses

The complete duration of all three records (CAMUS02, 17, and 19) was considered in sequence (one after another). It was considered, namely, that the damage from the previous tests (although it might not be visible from the exterior) might have an important influence on the stiffness as well as hysteretic behaviour of the wall. In figures only the requested time intervals (8s - 20s for CAMUS02; 5s-17s for CAMUS17; 5s - 17s for CAMUS19) are given. On diskettes, however, the response for the complete history of the relevant record is written.

2% of viscous damping, defined for the first natural mode, was used in the basic analyses.

Most typical results of the time-history analyses are given below:

- horizontal top displacement time history (Figure 17 - Figure 19),
- vertical top displacement (at the centre of the wall)time history (Figure 20 - Figure 22),
- top displacement versus base shear at the base of the 1st story (Figure 23 - Figure 25),
- hysteresis for the exterior spring at the 1st story (Figure 26 - Figure 28),

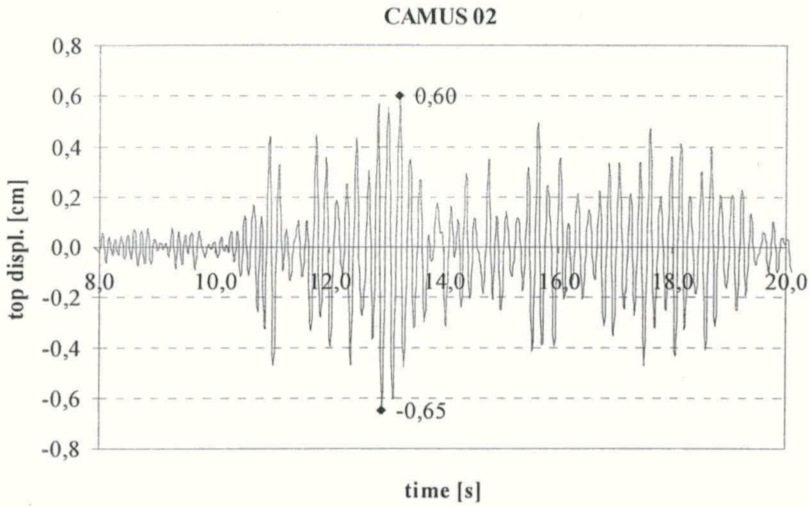

Figure 17 : Camus 02, horizontal top displ. time-history

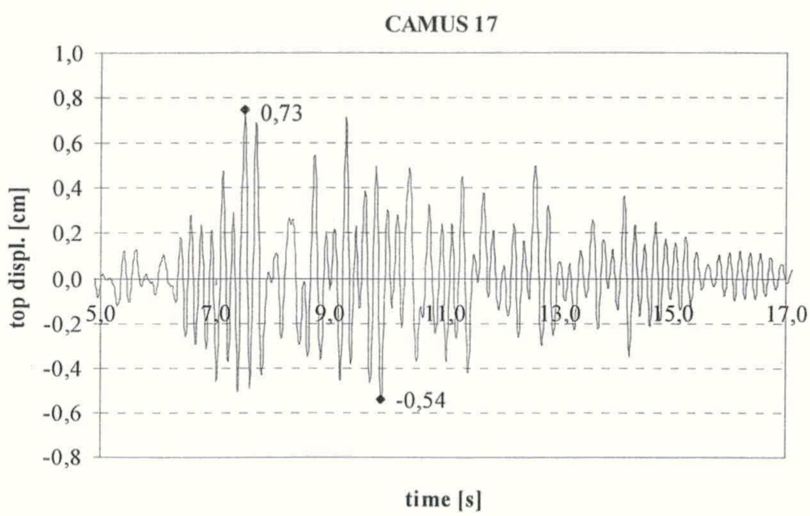

Figure 18: Camus 17, horizontal top displ. time-history

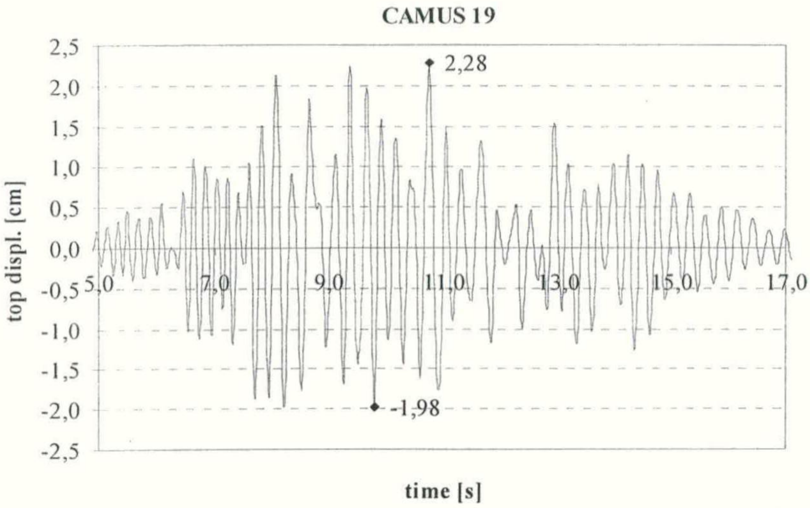

Figure 19: Camus 19, horizontal top displ. time-history

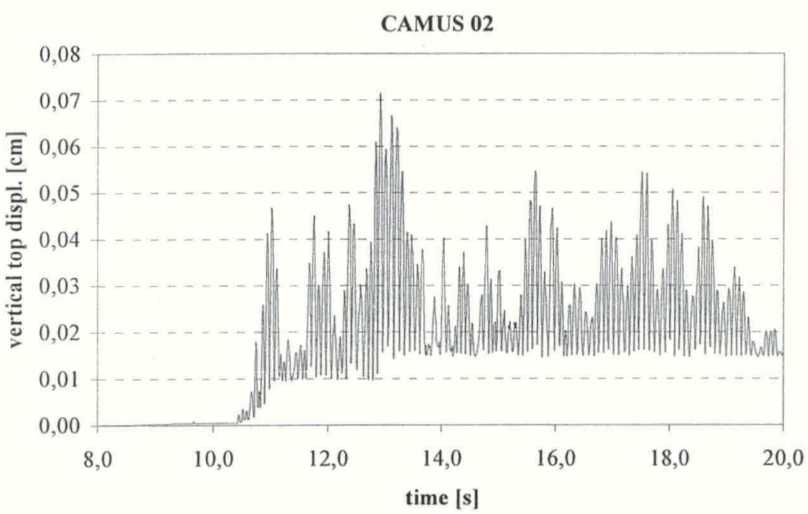

Figure 20: Camus 02, vertical top displacement

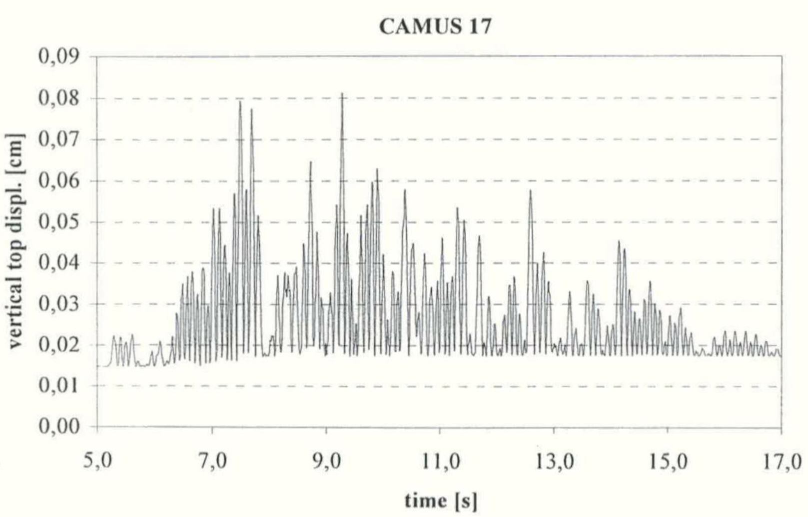

Figure 21: Camus 17, vertical top displacement

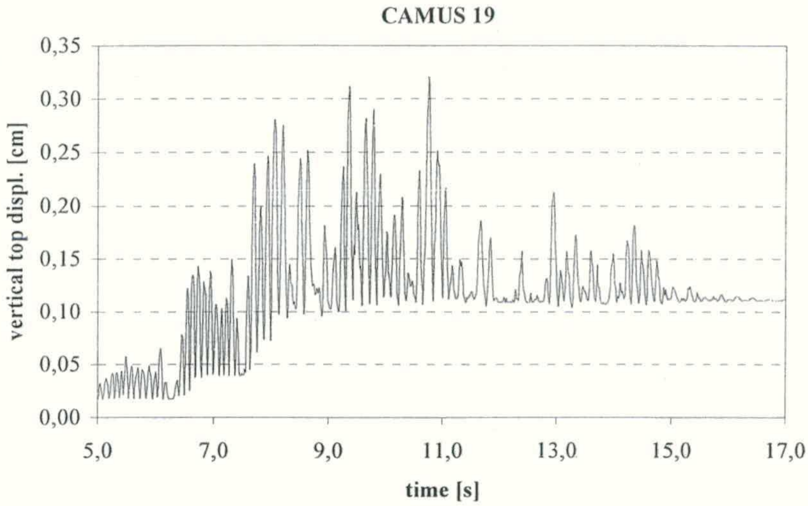

Figure 22: Camus 19, vertical top displacement

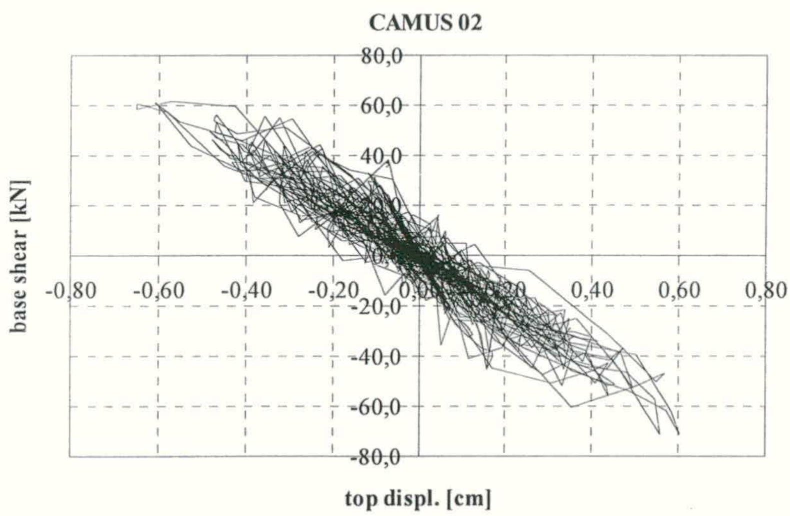

Figure 23: Camus 02, top displ. - base shear

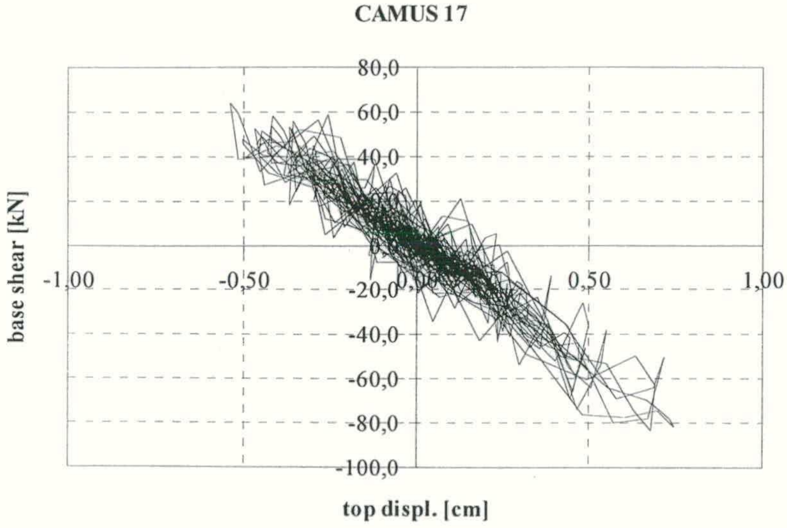

Figure 24: Camus 17, top displ. - base shear

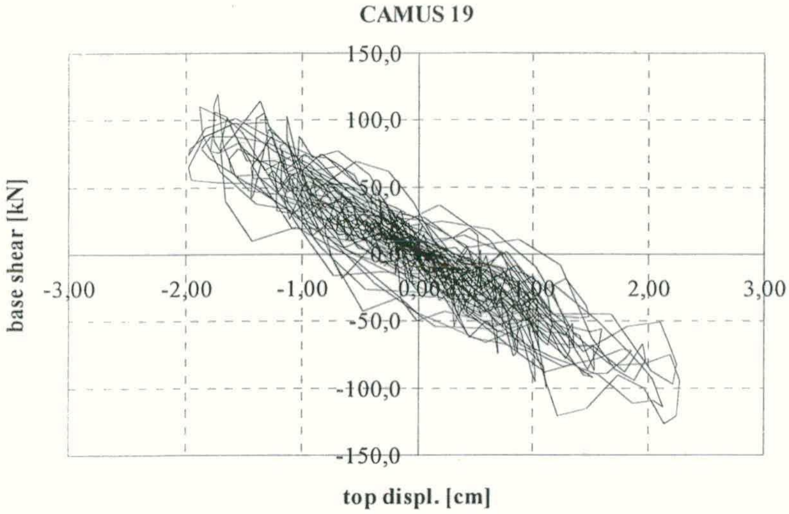

Figure 25: Camus 19, top displ. - base shear

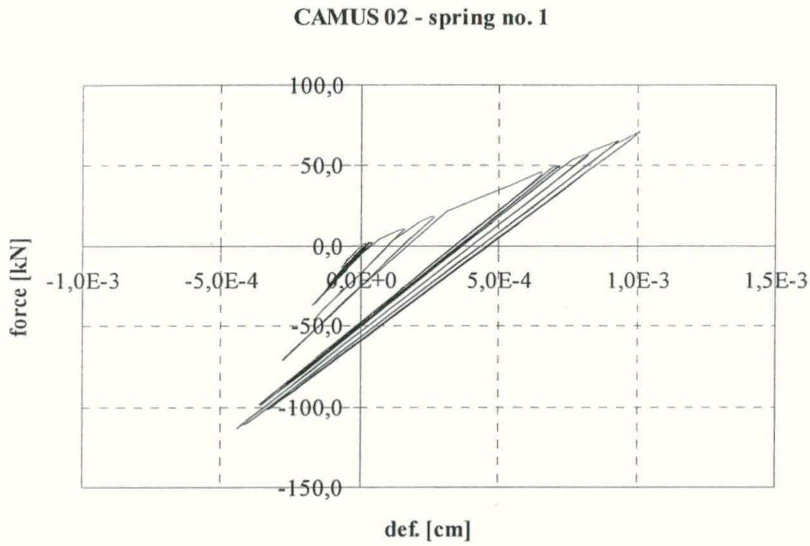

Figure 26: Camus 02, exterior spring hysteresis

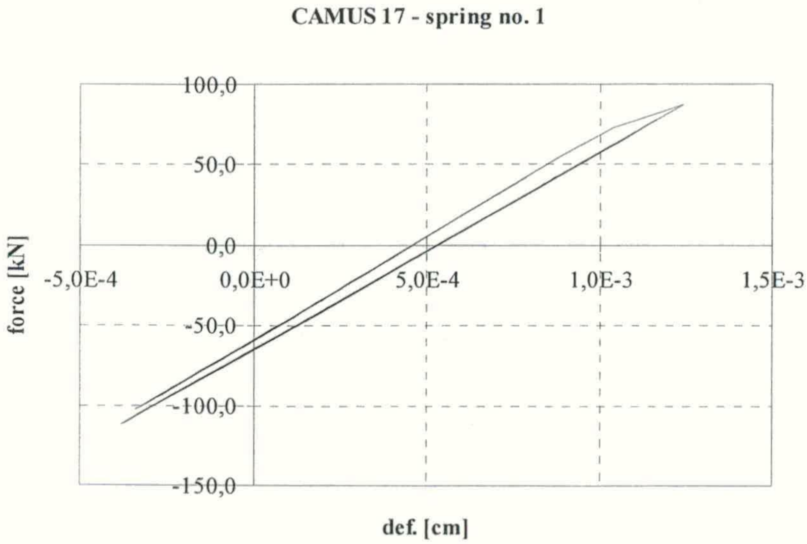

Figure 27: Camus 17, exterior spring hysteresis

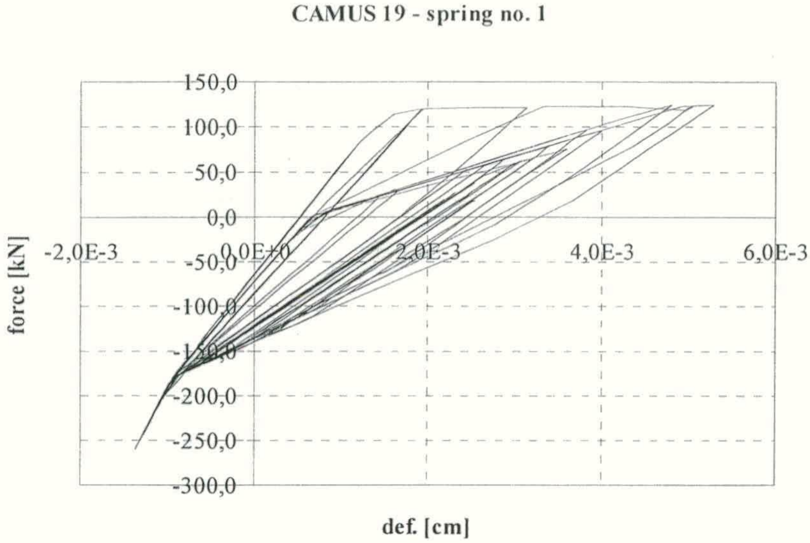

Figure 28: Camus 19, exterior spring hysteresis

7. COMPARISONS

Several comparisons were made to evaluate some of the main parameters used in the analyses.

7.1 Influence of damping

As expected, the choice of the damping coefficient has quite important influence on the response. This is particularly true for practically elastic response to Camus02 and Camus17 where there is no much hysteric damping. Therefore, the differences are particularly important at the end of the Camus17 record. In the case of the Camus19 record, the hysteric damping is more important and differences in the response obtained with 2% and 5% damping are relatively smaller.
Unfortunately, it is very difficult to assume the level of damping in advance and therefore this parameter may have an important influence on the errors in numerical prediction.

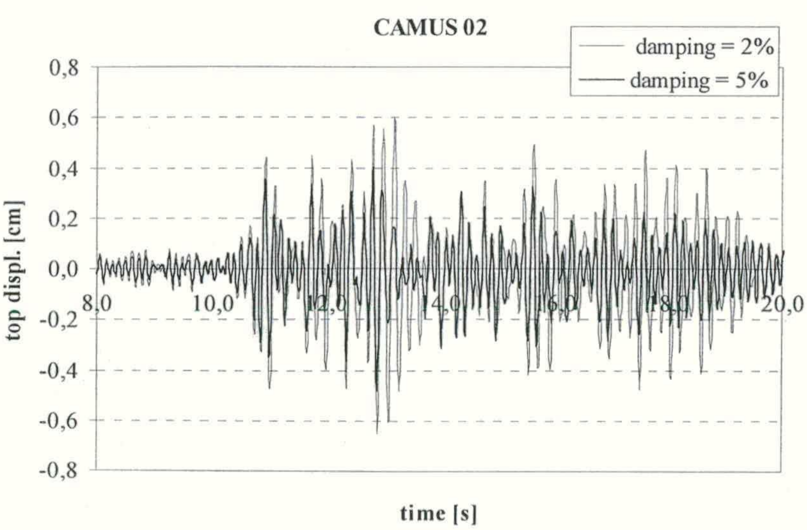

Figure 29: Camus 02, influence of damping

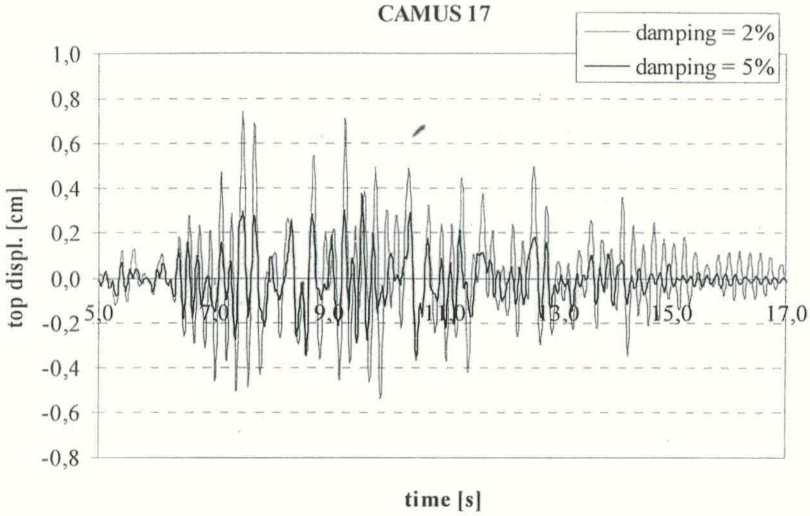

Figure 30: Camus 17, influence of damping

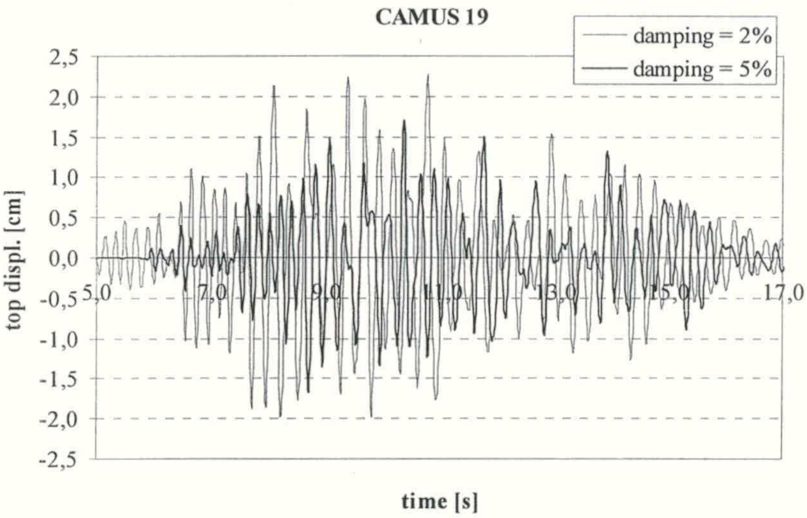

Figure 31: Camus 19, influence of damping

7.2 Influence of the reinforcement pull-out

The influence of the pull-out of the longitudinal reinforcement at the footing was investigated. Contact elements to simulate elastic and inelastic pull-out were added. Their characteristics were determined according to (Fillipou et al, 1992). Although we had expected different results, we were not able to indicate any important influence of the pull out on the displacement response.

7.3 Comparative analysis with the beam-column element

Cantilever structural walls have been frequently modelled with beam-column elements.

Although they are not able to simulate uplift of the wall, they should model adequately the horizontal displacement of an isolated cantilever wall. In our analysis, however, the differences between the results obtained with MVLE model and those, obtained by beam-column model were important (Figure 32 - Figure 35). It was concluded that the reason for that was different modelling of the behaviour in tension.

The MVLE model was very "soft" in tension since no tensile strength was assumed for concrete. However, the cracking moment in the beam-column element was considerable. This is clearly indicated by the results of the push-over analysis (Figure 32). If the cracking moment was reduced (to account for pre-cracking for example), the correlation with the MVLE was much better.

During the inelastic Camus19 response (Figure 35) a permanent shift was observed using beam-column elements. After yielding, the stiffness of the wall was small and the numerical response was difficult to control.

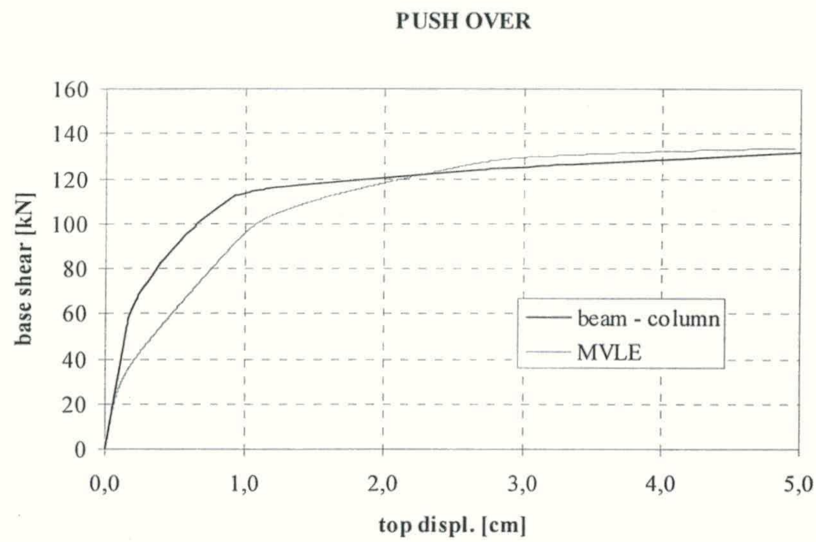

Figure 32: Push over, comparison with the beam-column element

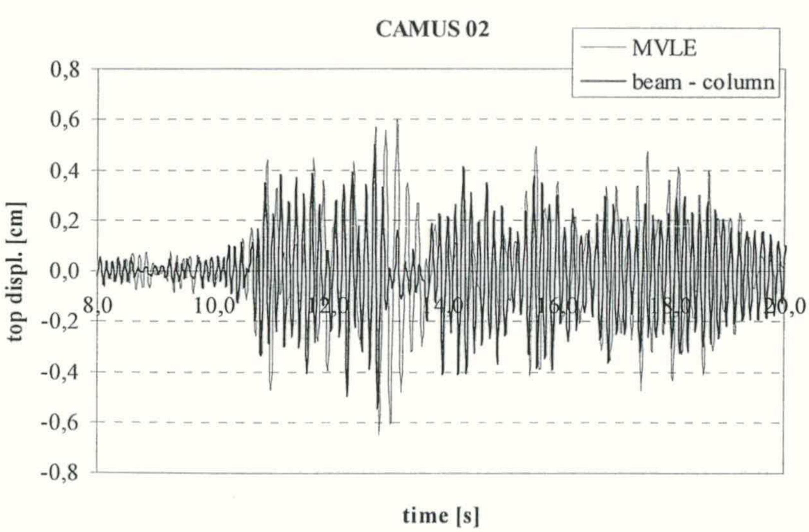

Figure 33: Camus02, comparison with the beam-column element

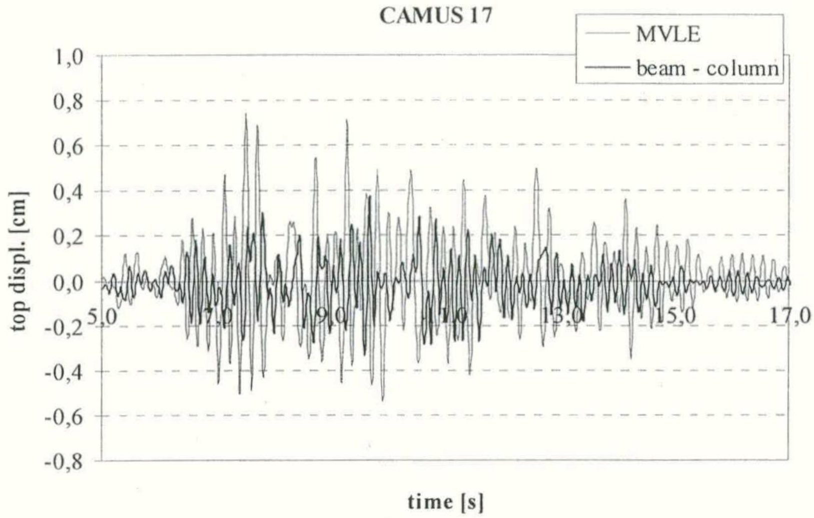

Figure 34: Camus17, comparison with the beam-column element

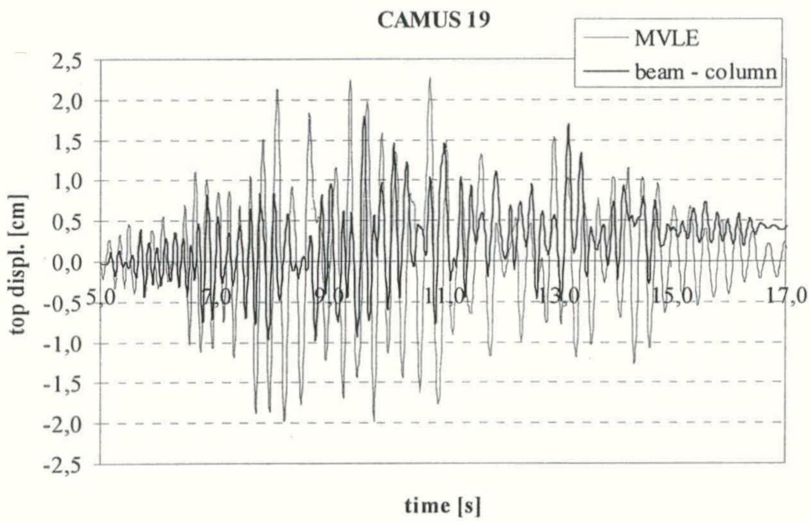

Figure 35: Camus19, comparison with the beam-column element

7.4 Comparative analysis with the N2 method

A simplified non-linear method (N2) has been developed at the University of Ljubljana (Fajfar, 1996). It combines non-linear static analysis (push-over) of the MDOF system and non-linear dynamic analysis of an equivalent SDOF system. Inelastic spectra can be conveniently used in dynamic analysis. This method was used to estimate the maximum horizontal displacement in the case of Camus19 response. The correlation of the calculated value (2,88 cm) with the result of the inelastic time-history analysis (2,28 cm) is acceptable, regarding all the uncertainties in the analysis.

7.6 Sequence versus individual records

Although not visible from outside, the damage/cracking from the previous test may have an important influence on the response of the subsequent test. Comparison in Figure 36 and Figure 37 confirms this statement. It had been decided, therefore, that the sequence of all three records was used in the basic analysis.

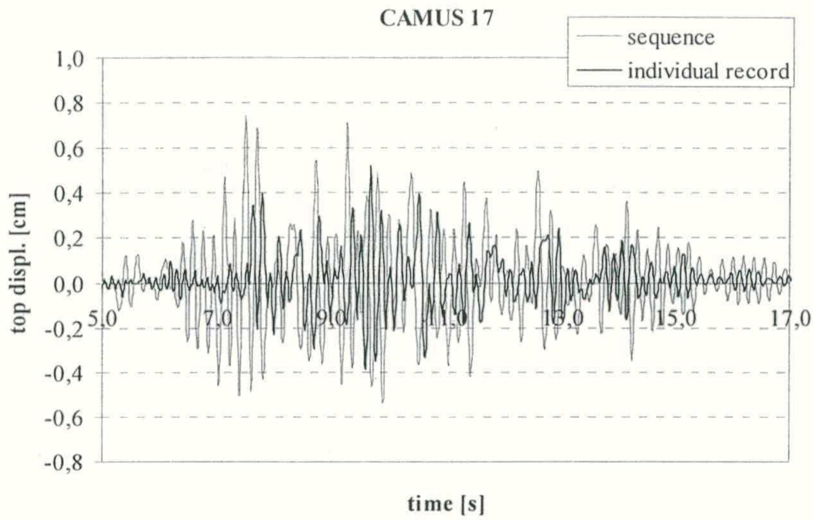

Figure 36: Camus 17, sequence versus individual record

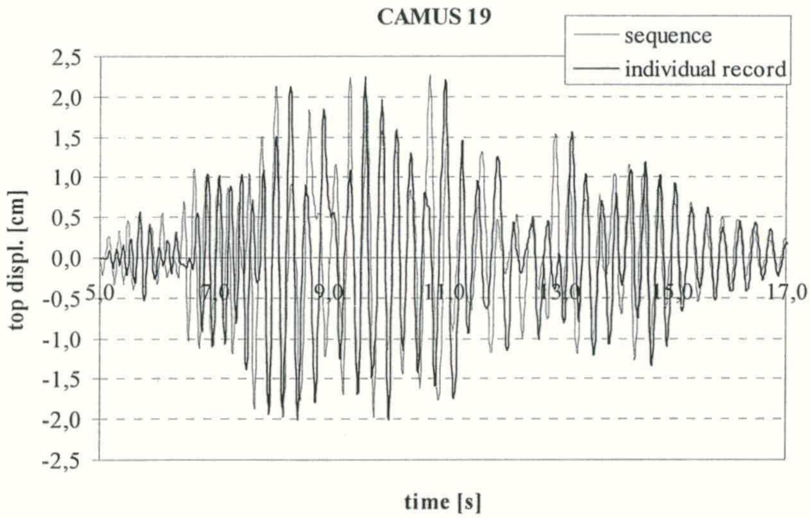

Figure 37: Camus 19, sequence versus individual record

7.7 Failure estimation

To obtain some notion of the failure capacity of the wall, the intensity (maximum ground acceleration) of the Camus19 record was increased. It was observed, however, that the system is quite unstable after yielding. Therefore, a minor increase of the ground acceleration (to 0.8g) caused the failure of the wall. The authors realise, that this could also be attributed to numerical instability and that the results strongly depend on the assumed hardening. In any case, the system is quite sensitive after yielding and any precise prediction of failure is difficult.

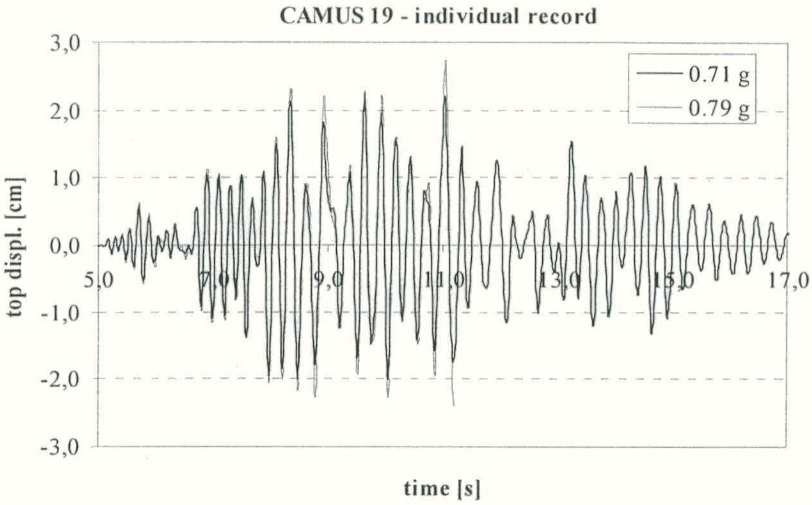

Figure 38: Failure estimation

8. CONCLUSIONS

The elastic strength of the analysed wall was high (it was concluded that no seismic force reduction was considered in the design and that some additional overstrength was provided by the choice of the reinforcement). Therefore, no yielding was observed in the response to Camus02 (cracking was quite intensive, however).
Although Camus17 seemed stronger (higher maximum ground acceleration), it was actually the weakest signal (see response spectrum). Therefore, no yielding was observed in the case of the response to Camus17, too.
Only Camus19 with very high maximum ground acceleration (0.71g) was strong enough to cause considerable yielding of the wall.

Immediately after yielding, the non-redundant single cantilever wall without distributed reinforcement became very weak and sensitive. The stability of the whole system depended strongly on the strain hardening parameter, which was difficult to estimate.

Since the wall capacity closely followed the demand over the entire height of the wall, the yielding was not confined to the base of the wall. Although this is not in accordance with the present Eurocode philosophy, it might be in accordance with the fact that no special construction details had been applied at the base of the wall.

Some parameters, like viscous damping, sequence of the tests, and modelling the behaviour in tension were found to be important. The choice of the appropriate values for these parameters was difficult, however.

According to our modelling, neither the pull-out of the reinforcement at the base of the wall, nor the influence of the inelastic shear (not mentioned in the main body of the report) was found to be important.

In general, after all this exercise, we are even more convinced, that "exact" prediction of the details of response is not feasible and that it depends on mere luck. We hope,

however, that predictions of global response parameters within the limits of several 10% are possible, and that should be considered as a good result.

REFERENCES

Fischinger, M., Vidic, T., Fajfar, P., Non-linear seismic analysis of structural walls using the multiple-vertical-line-element model. Paper presented at the workshop "*Non-linear Seismic Analysis and Design of Reinforced Concrete Buildings*", Bled, Slovenia. Proceedings (edited by Peter Fajfar and Helmut Krawinkler), pp.191-202, 1992.

'CAMUS' International Benchmark, Report I, Mock-up and loading characteristics. Specifications for the participants report, Commissariat a l'Energie Atomique, GEO and AFPS, 1997.

Earthquake resistant regulations, A world list - 1996, International Association for Earthquake Engineering, 1996.

Fafar, P. (Editor), Towards a new seismic design methodology for buildings - Research at the University of Ljubljana, IKPIR, 1996.

Fillipou, C.F., D'Ambrisi, A., Issa, A., Nonlinear static and dynamic analysis of reinforced concrete subassemblages, Report No. UBC/EERC-92/08, University of California, Berkeley, 1992.

Kanaan, A.E. and Powell, G.H., DRAIN-2D, A general purpose computer program for dynamic analysis of planar structures, Report No. UBC/EERC-73/6, University of California, Berkeley, 1973.

APPENDIX: Non-linear seismic analysis of structural walls using the multiple-vertical-line-element model. Paper presented at the workshop "*Non-linear Seismic Analysis and Design of Reinforced Concrete Buildings*", Bled, Slovenia. Proceedings (edited by Peter Fajfar and Helmut Krawinkler), pp.191-202, 1992.

NONLINEAR SEISMIC ANALYSIS OF STRUCTURAL WALLS USING THE MULTIPLE-VERTICAL-LINE-ELEMENT MODEL

MATEJ FISCHINGER, TOMAŽ VIDIC, PETER FAJFAR
University of Ljubljana, Department of Civil Engineering,
Institute of Structural and Earthquake Engineering,
Jamova 2, 61000 Ljubljana, Slovenia

ABSTRACT

The multiple-vertical-line-element model (MVLEM) has been applied to the inelastic static and dynamic response analysis of structural walls. Three different structural systems (a cantilever wall, a frame-wall building, and a coupled wall) were selected as illustrative examples. A comparison of analytical and experimental results indicates that the MVLEM can successfully predict the inelastic behaviour of all three different types of structural walls. The main advantage of this model is its ability to simulate the shift of the neutral axis (due to the lifting of the tension edge of the wall after yielding) and to take into account the influence of a fluctuating axial force on the strength and stiffness of the wall. Both of these features are particularly important in the case of coupled wall systems. There are, however, several problems which need further investigation. They include (i) the modeling of inelastic shear behaviour, (ii) refinement of the models for vertical springs, (iii) the calibration of the model parameters and (iv) the formulation of a new model for coupling beams.

INTRODUCTION

Properly designed and correctly constructed reinforced concrete (RC) structural walls may, in addition to their high strength, exhibit very high ductility. Due to their stiffness, they reduce the seismic damages of non-structural systems. Consequently, they are very effective in providing safe and sound structural systems in earthquake regions. Unfortunately, the present capability for the realistic and practical mathematical modeling of the nonlinear static and dynamic seismic response of RC structural walls is limited. Among many proposed models, which have been discussed for example in [1], the multiple-vertical-line-element model (MVLEM) has gained a lot of interest lately, and the model is believed to be reasonably reliable in the seismic analysis of RC buildings with structural walls (e.g. [2,3]). In the paper, the basic concepts of the MVLEM are discussed and its effectiveness has been analysed by illustrative examples for three different types of structural walls.

THE MULTIPLE-VERTICAL-LINE-ELEMENT MODEL (MVLEM)

The physical model

Following the full-scale test carried out on a seven story RC frame-wall building in Tsukuba (U.S. - Japan program [4]), Kabeyasawa et al [2] proposed a new macroscopic three-vertical-line-element model (Fig. 1). In the model three vertical elements are connected by rigid beams at the top and bottom floor levels. Two outside truss (uniaxial) elements represent the axial stiffness of the boundary columns. The central vertical element, representing the panel of the wall, is a one-component model in which the vertical, horizontal and rotational springs are concentrated at the base. Since it is difficult to assign justifiable values to the rotational spring, a modified model (Fig. 2) was proposed by Vulcano et al [3]. The rotational spring was replaced by several (N) parallel vertical truss elements, which represent the axial and flexural stiffness of the central panel. The horizontal spring, which models the shear behaviour of the wall member, has remained in the model. This model is called the multiple-vertical-line-element model (MVLEM). It was incorporated into the DRAIN-2D program by the authors and used in the present study.

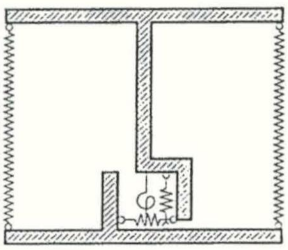

Figure 1. Three-vertical-line-element model (TVLEM) [2]

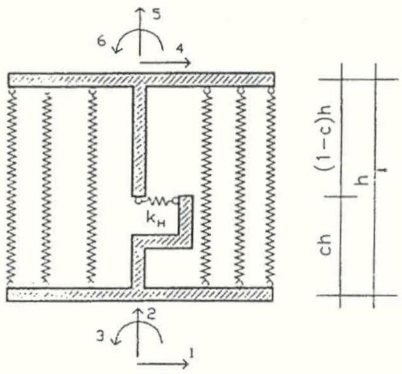

Figure 2. Multiple-vertical-line-element model (MVLEM) [3]

The entire wall is modeled as a stack of n MVLEM wall elements which are placed one upon each other. The flexural and shear deformations are separated in each MVLEM (Fig. 3). All shear behaviour is concentrated in the horizontal spring with stiffness k_H, which is placed at the height ch ($0 \leq c \leq 1$). The horizontal shear displacement at the top of the stack does not depend on c. Flexural deformations, however, do depend on c, as well as on n. The parameter c defines the relative rotation between the top and bottom levels of the MVLEM (Fig. 3). If moment (curvature) distribution along the height of the element is constant, $c = 0.5$ yields "exact" rotations and displacements for elastic and inelastic behaviour. For a triangular distribution of bending moments, $c = 0.5$ still yields exact results for rotations in elastic range, but it underestimates displacements. This problem can be solved by the stacking of elements, which leads to a small moment gradient. In the inelastic range, however, the problem is more critical, since even small moment gradients can cause highly nonlinear distributions of curvature. Consequently, lower values of c should be used to take into account the non-linear distribution of curvature along the height of the wall. For the analysed multistory walls, good results were obtained if: (i) 3 to 4 MVLEM's were used in the potential hinge area (the first story) and $c = 0.3$ was chosen.

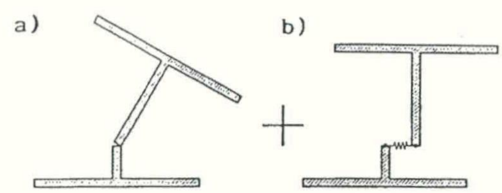

Figure 3. Flexural (a) and shear (b) deformations of the MVLEM

Hysteretic models

Based on the results of the test in Tsukuba, Kabeyasawa [2] proposed a special axial force - deformation formulation for vertical springs. Similar, though simplified, hysteretic rules, which had been originally developed by the authors for the contact elements in the joints of large panel buildings, were used in the present examples (Fig. 4). Modeling of inelastic shear behaviour has not yet been appropriately solved. Simplified rules were included into the MVLEM by the authors (Fig. 5). In the present study, inelastic shear behaviour was considered in the case of the cantilever wall only.

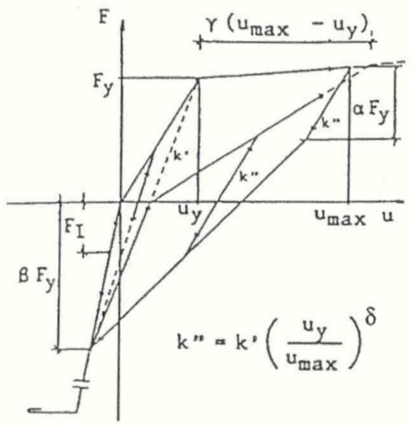

Figure 4. Vertical spring behaviour

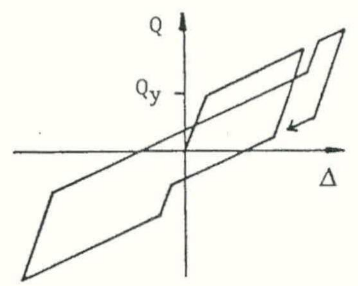

Figure 5. Horizontal spring behaviour

THE MODELING OF COUPLING BEAMS

The response of a coupled wall depends strongly on the behaviour of the coupling beams, which is specific and different from that of beams in frames. The typical behaviour of a conventionally reinforced coupling beam is shown in Fig. 6. During the first half cycle a crack opens on one side (e.g. at the top) (Fig. 6a). During the second half cycle it may happen that the crack at the bottom opens before the one on top closes. In such a case a gap spreads over the entire height of the coupling beam (Fig. 6b), which is associated with moment capacity reduction and shear-slip. As well as this, the lugs of the deformed reinforcement cause localized crushing of the concrete in the first half cycle. This would cause the development of the voids behind the lugs. When the direction of loading in the

beam is reversed, the reinforcement must slip the distance of the voids before the lugs can bear on their opposite faces. Furthermore, large deformation demands are imposed on the beams after yielding of the adjacent tension edge of the wall pier which tends to uplift. In such a case it is practically impossible to avoid slip between the conventionally reinforced beam (without diagonal reinforcement) and the pier (see also Fig. 14). Finally, if the deformation in the reloading cycle is large enough, the gap closes and the stiffness increases (Fig. 6c).

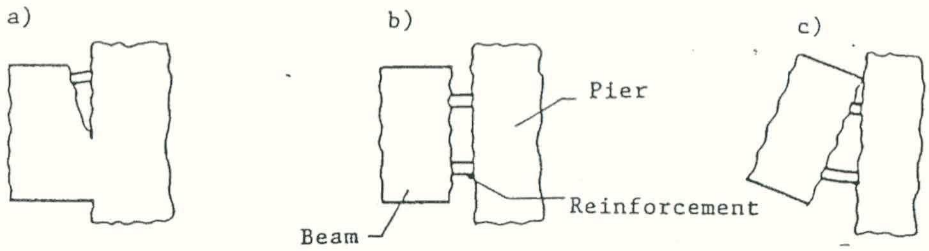

Figure 6. Behaviour of a coupling beam: (a) first crack, (b) crack opens over the entire height, (c) gap closure

A simple model has been proposed to simulate the observed behaviour (Fig. 7a). Springs following shear-slip hysteretic rules (Fig.7c) were placed between the beam and the piers (notē that similar were used to model shear behaviour in the MVLEM). With these springs, the level of the shear force in the beam (the axial force in the piers) can be controlled and the slip associated with the uplift of the piers can be modeled. The rotational degrees of freedom in the contacts between the springs and beam (nodes 3 and 4) are fixed, which results in the deformation mode illustrated in Fig. 7b. Consequently, the inflexion point still occurs in the middle of the beam, as has been supposed by most researchers in the past.

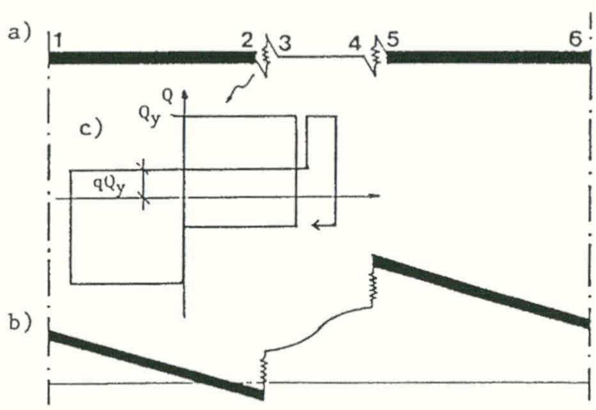

Figure 7. Proposed model for coupling beams: (a) undeformed configuration, (b) deformed configuration, (c) hysteretic rules for the shear springs

EXAMPLE No. 1: A CANTILEVER WALL

The analytical results [1] were compared with the results of a test on a simple cantilever wall with a rectangular cross-section (Fig. 8). The test was conducted at Tsinghua university in Beijing. The height of the wall was 2.4 m, the cube strength of the concrete was 36.0 MPa and the yield strength of reinforcement was either 381 MPa (ϕ 12 mm bars) or 288 MPa (ϕ 8 mm bars). The wall was subjected to cyclic loading. A MVLEM was used in the analysis. The analytical and test results agreed well for the following set of parameters: $n = 8$, $N = 6$, $c = 0.3$, $\alpha = 1.0$, $\gamma = 1.05$ and $\delta = 0.5$. The response was very much influenced by the parameter β, which determined the "fatness" of the hysteresis of the vertical springs. It had to be defined by a trial and error procedure. The relation $\beta = 1.5 + F_I / F_y$ was adopted, where F_I and F_y were the initial compression force and the yield force in the spring, respectively. For comparison two other mathematical models were used: (i) a simple equivalent beam model and (ii) a finite element model (FEM) [5]. The following was concluded:

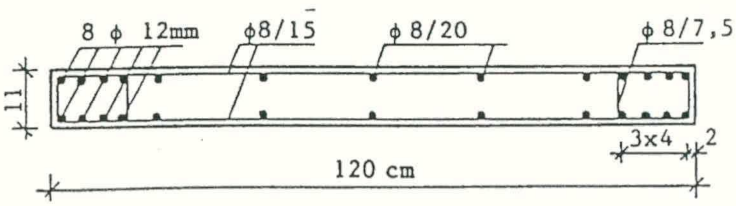

Figure 8. Cross-section of the cantilever wall

1. As far as the global response relation top displacement - base shear is concerned, the simple beam element simulated the response as successfully as the MVLEM. This is not surprising, since the moment - rotation relationship for flexural behaviour of the beam element can be relatively reliably determined (in fact more approximations were used in the case of the MVLEM).
2. A larger discrepancy was observed in the case of the FEM. One reason for this might be the perfect bond between the steel and concrete, which was enforced in the model. This proves once again that FE models often depend on parameters which are difficult to define or control. It should be noted, however, that in the MVLEM the parameter β was adjusted while the parameters in the FEM were not.

EXAMPLE No. 2: A 7-STORY FRAME-WALL RC BUILDING

The well-known 7-story RC dual building tested at full scale in Tsukuba (Japan) offers an ideal example to test the efficiency of the chosen mathematical model. The floor-plan and cross-section of the building are shown in Fig. 9. A detailed description of the building has been published in many reports (e.g. [4]) and so will not be repeated here.

The building was analysed by the authors of this paper by using a simple equivalent beam element for the structural wall. Fair correlation of the measured and computed overall response of the structure, expressed, for example, in terms of the top displacement time-history, was observed (Fig. 10) [6]. The correlation of the detailed response, however, was not so favourable. A large discrepancy was observed in the lower part of the displacement envelope (Fig. 11), where the measured displacements were much larger than the computed

ones. According to the analysis, the columns did not yield at the base, although the results of the test indicated plastic hinges at the column base. In addition to this, some parameters of the beam element model (e.g. the hardening slope) had to be based on the test results.

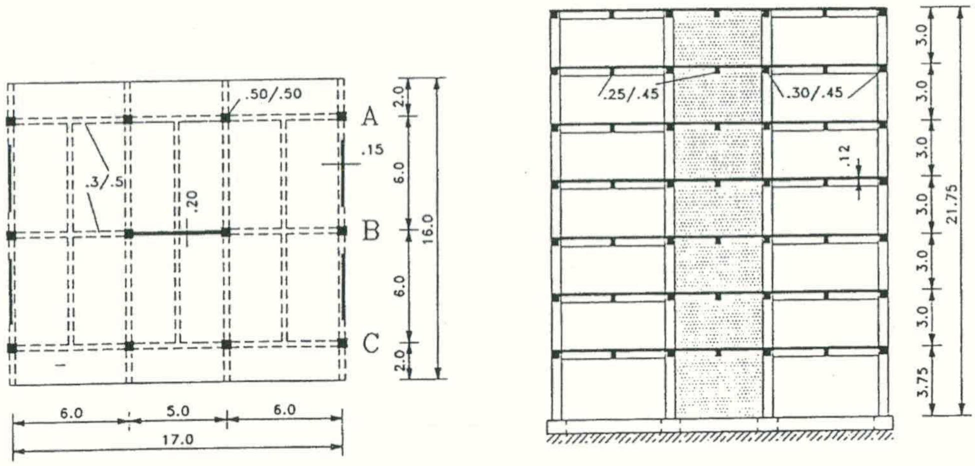

Figure 9. Plan and vertical section of the "Tsukuba" building [4].

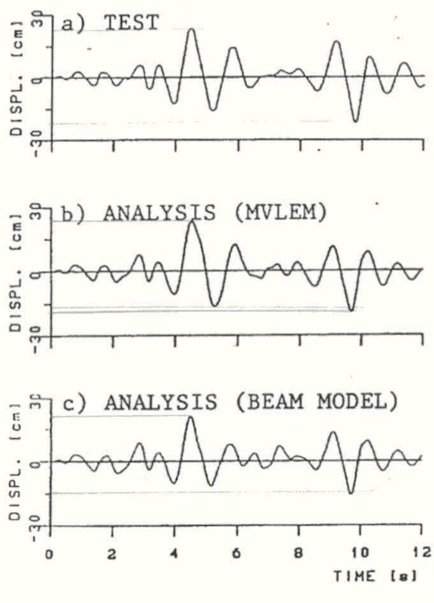

Figure 10. Top displacement time history for the "Tsukuba" building: (a) test, (b) MVLEM, (c) beam model

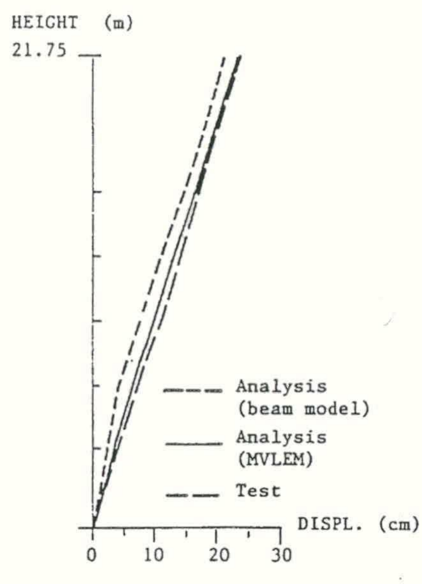

Figure 11. Displacement envelope for the "Tsukuba" building: Comparison of test and analyses

The inelastic response of the same building to the PSD-3 loading was recalculated by using the MVLEM for the structural wall [7]. Three elements were used in the first floor and one element in each of the other floors. Six vertical springs were employed in all the

elements. The location of the horizontal spring was defined by the parameter $c = 0.3$. Elastic behaviour of all shear springs was assumed. The following parameters were used to control the response of the wall elements: $\alpha = \beta = \gamma = 1.0$ and $\delta = 0.5$. The strain hardening ratio of the beam vertical springs in tension was 0.01. The modeling of columns and beams was, with a small exception of beams subjected to a negative bending moment (tension at the top), the same as that for previous models in the analysis. Additional springs were used to simulate the three-dimensional behaviour of the building (the influence of the transverse beams). The accelerogram which was applied in Test PSD-3 in Tsukuba was based on the E-W component of the Taft record (1952). The maximum ground acceleration was 320 cm/s^2.

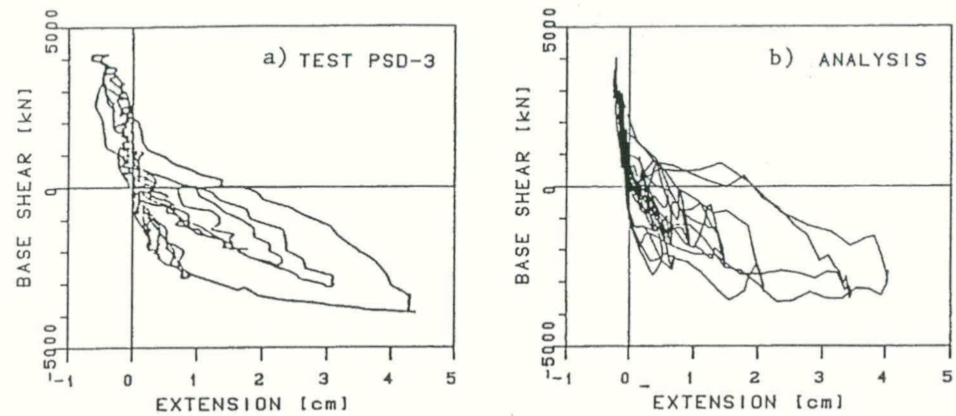

Figure 12. Extension of the right boundary column in the first story of the "Tsukuba" building: (a) test, (b) MVLEM

Some results of the analysis are shown in Figs. 10-12. The correlation between the measured and computed values is favourable not only in the case of the top displacement time-history (Fig. 10), but also in the case of the axial deformation of the boundary column of the wall (Fig. 12) and of the building's displacements envelope (Fig. 11). The results have proved that the MVLEM was capable of simulating the detailed response of the wall, which controlled the overall response of the tested building. Note also that some differences arise from the fact that MDOF model was used in the analysis, while SDOF response had been enforced in the test. The same failure mechanism as that observed in Tsukuba was predicted.

EXAMPLE No. 3: A COUPLED WALL

A 6-story coupled structural wall (Fig. 13), which was tested by Lybas and Sozen [8], was chosen as the third example. The choice was partly based on the excellent documentation of the results as well as of the input data. A total of six small-scale structures were tested. Five test structures were subjected to the scaled El Centro NS motion and one structure (speciment S1) was subjected to cyclic lateral loads. For example, the crack pattern after the cyclic test is shown in Fig. 14.

Only the preliminary results for specimen S1 (referred to as the "coupled wall" in the following text) are given below. Lybas and Sozen used a simple beam element, which disregarded axial force - flexural interaction, to model the piers of the coupled wall. An

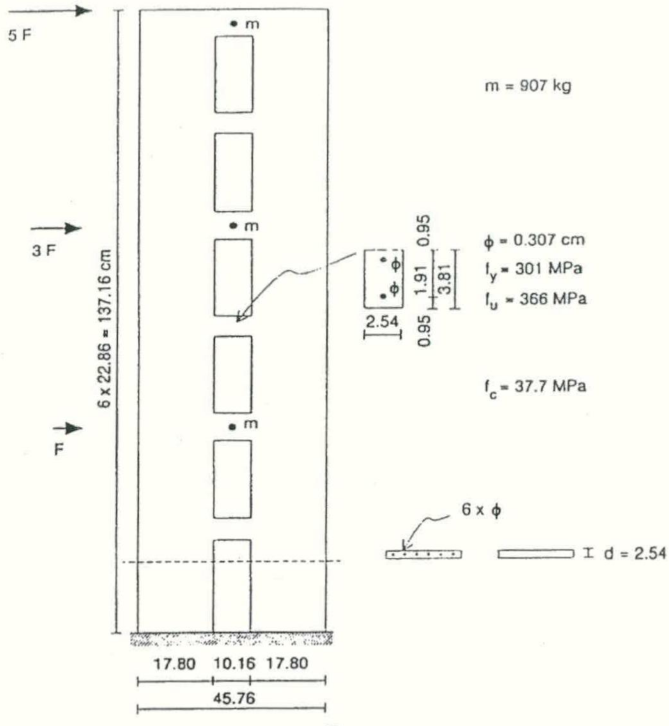

Figure 13. The coupled wall

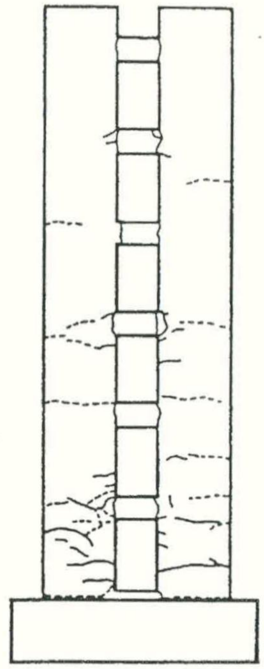

Figure 14. Crack pattern after the cyclic test [8]

extensive parametric study was performed to define a suitable model for the coupling beams. It was necessary to modify the original Takeda rules to account for shear-slip, the slip of the longitudinal reinforcement in the beams, and gap closure in the reloading cycle. A line element which included axial force - flexural interaction was used by Keshavarzian and Schnobrich [9] to model the wall piers of the same coupled wall. They reported that the interaction did not affect the overall response (stiffness) of the wall. However, yielding of the tension pier did change the distribution of the bending moment between the two piers, as well as the distribution of shear. In the present study, both, modified beam behaviour and axial force - flexural interaction have been taken into account. In addition, the uplift of the tension edges of the piers has been considered.

Four different models (A - D) were used in the analysis and the results were compared with the experimentally observed top level load - top level lateral deflection relation of the wall when subjected to cyclic lateral loads (Fig. 15e). In all the models four MVLEM's were used in the first story of both piers and one MVLEM was used in each of all the other stories. The parameters $N = 6$, $c = 0.3$, $\alpha = 1.0$, $\gamma = 1.0$ and $\delta = 0.5$ were used throughout the analysis. One percent of hardening after yielding was assumed for the vertical springs in the MVLEM. Details of the individual models are discussed below.

Model A

1. The coupling beams were modeled as simple beams following the original Takeda rules.
2. The moment - rotation envelope for the beams was based on the assumed antisymmetric distribution of moment and curvature. The yield moment ($M_y = 5.6$ kNm) and ultimate moment ($M_u = 7.2$ kNm) were calculated. The calculated ultimate moment was lower than that reported in [8] (8.81 kNm).
3. The calculated hardening slope for the beams was 2.7 %.
4. $\beta = 1.0$ was chosen in the MVELM.
5. The compressive axial stress in the vertical springs of the MVLEM was limited to 32 MPa = 0.85 f_c.

The correlation between the test and calculated results is poor (Fig. 15a). Large rotational ductility demand ($\mu_\Theta = 90$) was imposed on the coupling beams after the uplift of the adjacent tension edge of piers, which amounted to 0.5 cm (6 cm in the prototype structure). In reality, beams cannot sustain such a large ductility demand. In the applied model, however, the ductility was not limited and, due to the hardening in the post yield range, the bending moment in the beams increased up to 19.0 kNm. Consequently, the shear forces in the beams, the axial forces in the piers, the flexural capacity of the wall and the horizontal resistance of the wall increased unrealistically. Finally, the vertical springs of the MVLEM at the base yielded in compression. Detail "x" in the cyclic response (Fig. 15a) can be explained by an increase in the stiffness of the vertical springs which occurred after the force had fallen below the yield level again. The shear forces in the beams could be limited if a smaller hardening ratio in the beams was used. This "solution", however, has no physical background.

Model B:

While all the other parameters were kept constant, the proposed modified beam (Fig. 7) was used. The yield force of the shear spring was determined from the ultimate moment calculated for the coupling beam ($Q_y = 2\,M_u / L_b$, where L_b is the clear length of the beam). No degradation of the force in the shear springs was assumed (q = 1.0, Fig. 7c). The following can be observed (Fig. 15b):

1. In comparison with Model A, much better agreement was achieved.
2. The calculated horizontal force is lower than was observed during the test. However, if the (higher) values for the ultimate moment in beams, which had been reported in [8], were used, the correlation would be better.
3. A sudden increase in stiffness on the reloading branch (detail "xx"), which was not observed during the experiment, can be noted. This problem was further investigated by the other two models.

Model C

Model C was the same as Model B, except for the degradation of the force in the shear springs (q = 0.3). The general shape of the hysteresis loops was improved (Fig. 15c). Nevertheless, the mentioned stiffness increase persisted in them.

Model D

While all the other parameters of Model C were kept constant, the parameter β of the vertical springs in the MVLEM was determined according to the relation which had been proposed for the cantilever wall in Example 1 ($\beta = 1.5 + F_I \;/\; F_y = 2.5$). The observed

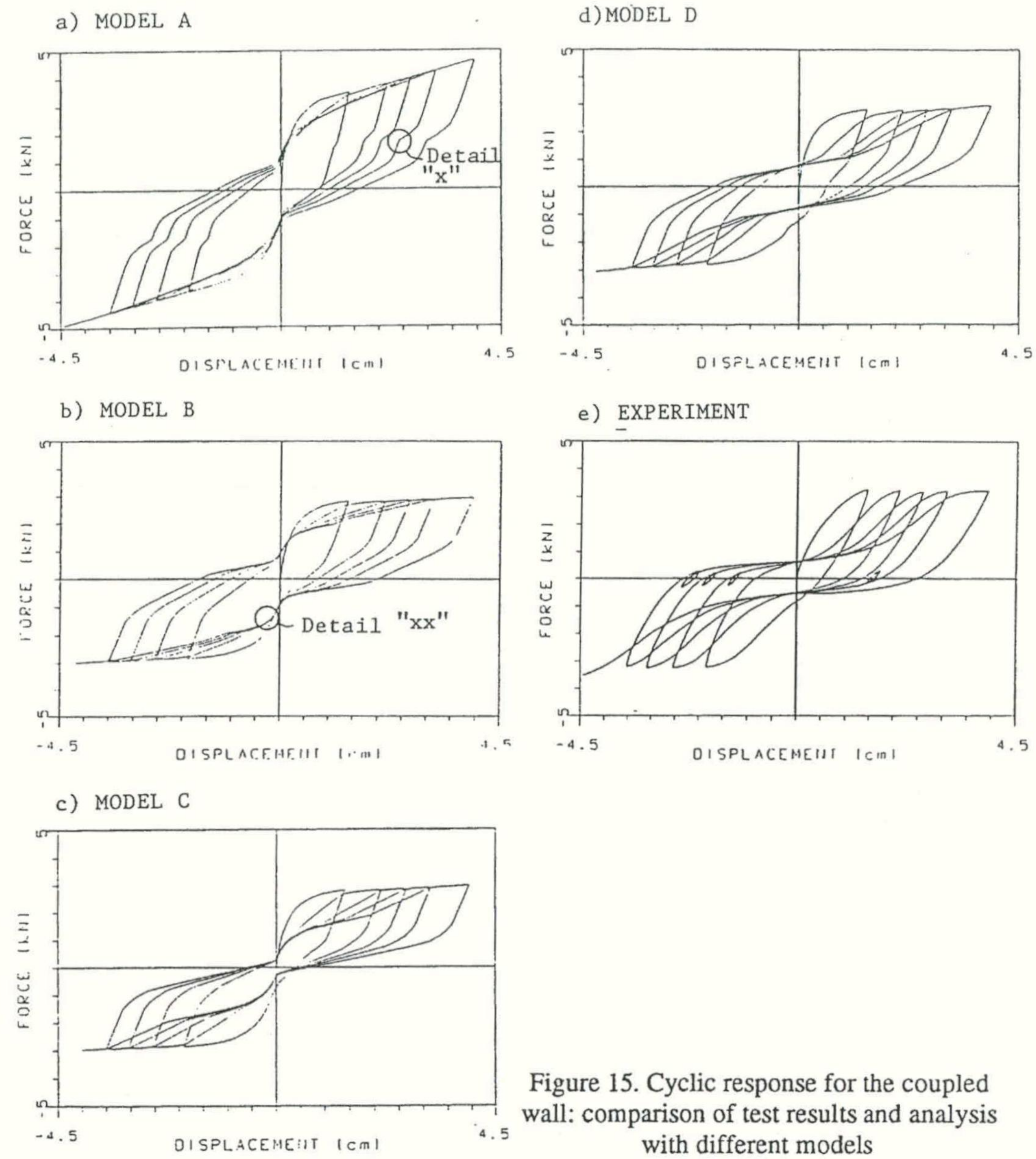

Figure 15. Cyclic response for the coupled wall: comparison of test results and analysis with different models

increase of stiffness vanished from the cyclic response hysteresis (Fig. 15d) and reasonable agreement with the test results was achieved. Noticable strength degradation, which was not successfully simulated, might be controlled by a larger γ value in the model for the vertical springs. However, this has not yet been verified.

CONCLUSIONS

1. The MVLEM quite successfully balances the simplicity of a macroscopic model and the refinements of a microscopic model. Its physical concept is clear, and the computational effort needed is reasonable. It enables modeling of some important features (e.g. shift of the neutral axis, the effect of a fluctuating axial force, inelastic shear behaviour) which have been frequently ignored in previous seismic analyses of structural walls.
2. The MVLEM was able to predict the inelastic static, cyclic and (in one case) dynamic behaviour of three different types of structural walls (a cantilever wall, a coupled wall and a frame-wall structural system).
3. While there was no particular advantage of the MVLEM over a simple beam model in simulating the global response (top displacement - base shear) of the cantilever wall, the advantages of the MVLEM were clearly seen in the case of the other two structural systems, where structural walls were connected with other elements which restrained their local deformations.
4. Successful simulation of the frame-wall interaction had been expected. After all, the basic concept of the model was proposed in accordance with the test results obtained for the analysed frame-wall building.
5. It is a new observation, however, that the MVLEM is particularly suitable for modeling coupled wall response. Moreover, the authors are convinced that a realistic estimate of the demand in coupling beams is not possible if the shift of the neutral axis and the influence of the fluctuating axial forces in the walls are not properly taken into account.
6. Vice versa, the behaviour of coupling beams controlled the response of the analysed coupled wall. Simple beam model, following the original Takeda hysteretic rules, was found inadequate to predict this behaviour at the large displacements imposed on the wall, associated with large vertical elongations of the tension edges of the coupled piers. A new model for coupling beams is therefore needed. In the presented analysis shear slip elements were added to the interfaces of the coupling beams and wall piers.
7. The behaviour of all the analysed walls was predominantly flexural and the level of the axial forces was relatively low. To account for the highly inelastic shear behaviour better models are needed. If the level of compressive axial forces was higher, nonlinear behaviour (including the confining effect) of the vertical springs in compression should be taken into account.
8. Some of the model parameters (in particular c and β) have an important influence on the response. Recommendations for their values are given in the paper. They need, however, further calibration.

ACKNOWLEDGEMENTS

The results presented in this paper are based on work supported by the Ministry of Research of the Republic of Slovenia and by the U.S. - Yugoslav Joint Fund for Scientific and Technological Cooperation.

REFERENCES

1. Fajfar, P. and Fischinger, M., Mathematical modeling of reinforced concrete structural walls for nonlinear seismic analysis. In Proc. of the European Conf. on Struc. Dyn., EURODYN '90, Bochum, Germany, A.A. Balkema, 1991, pp. 471-78.
2. Kabeyasawa, T., Shiohara, H., Otani, S. and Aoyama, H., Analysis of the full-scale seven-story reinforced concrete test structure. Journ. of the Fac. of Eng., Univ. of Tokyo, 1983, 37, pp. 431-78.
3. Vulcano, A., Bertero, V.V. and Colloti, V., Analytical modeling of R/C structural walls. Proc. 9th WCEE, Tokyo - Kyoto, Maruzen 1989, Vol. 6, pp. 41-46.
4. U.S. - Japan Cooperative Research Programs, Test of reinforced concrete structures, Proc. 8th WCEE, San Francisco, Prentice Hall, 1984, Vol. 6, pp. 593 - 706.
5. Damjanić, F.B., Finite element modelling in structural reinforced concrete analysis. In Nonlinear Seismic Analysis of Reinforced Concrete Buildings, eds. P. Fajfar and H. Krawinkler, Elsevier, 1991.
6. Fajfar, P. and Fischinger, M., Nonlinear seismic analysis of RC buildings. Implications of a case study. European Earthquake Engineering, 1987, 1, pp. 31-43.
7. Fischinger, M., Vidic, T. and Fajfar, P., Evaluation of the inelastic response of a R.C. building with a structural wall designed according to Eurocode 8. In Proc. of Int. Conf. Buildings with Load Bearing Concrete Walls in Seismic Zones, Paris, 1991, pp. 487-98.
8. Lybas, J.M. and Sozen, M.A., Effect of beam strength and stiffness on dynamic behaviour of reinforced concrete coupled shear walls. Report No. SRS 444, University of Illinois at Urbana - Champaign, 1977.
9. Keshavarzian, M. and Schnobrich, W.C., Computed nonlinear seismic response of R/C wall-frame structures. Report No. SRS 515, University of Illinois at Urbana - Champaign, 1984.